SIRIUS-M: A Symmetric Illumination, Inertially Confined Direct Drive Materials Test Facility

B. Badger, S.I. Abdel-Khalik, H.M. Attaya, R.L. Engelstad, G.L. Kulcinski, E.G. Lovell, G.A. Moses, Z. Musicki, R.R. Peterson, M.E. Sawan, I.N. Sviatoslavsky, L.J. Wittenberg

October 1987

UWFDM-729

FUSION TECHNOLOGY INSTITUTE

UNIVERSITY OF WISCONSIN

MADISON WISCONSIN

SIRIUS-M: A Symmetric Illumination, Inertially Confined Direct Drive Materials Test Facility

B. Badger, S.I. Abdel-Khalik, H.M. Attaya, R.L. Engelstad, G.L. Kulcinski, E.G. Lovell, G.A. Moses, Z. Musicki, R.R. Peterson, M.E. Sawan, I.N. Sviatoslavsky, L.J. Wittenberg

Fusion Technology Institute
University of Wisconsin
1500 Engineering Drive
Madison, WI 53706

http://fti.neep.wisc.edu

October 1987

UWFDM-729

DOE/DP10613

SIRIUS-M: A SYMMETRIC ILLUMINATION, INERTIALLY CONFINED DIRECT DRIVE MATERIALS TEST FACILITY

B. Badger, S.I. Abdel-Khalik, H.M. Attaya, R.L. Engelstad,
G.L. Kulcinski, E.G. Lovell, G.A. Moses, Z. Musicki,
R.R. Peterson, M.E. Sawan, I.N. Sviatoslavsky, L.J. Wittenberg

Fusion Technology Institute
University of Wisconsin
1500 Johnson Drive
Madison, WI 53706-1687

October 1987

TABLE OF CONTENTS

EXECUTIVE SUMMARY

SIRIUS-M is a study of a uniformly illuminated ICF materials test facility performed by the Fusion Technology Institute of the University of Wisconsin (FTI) in collaboration with the University of Rochester's Laboratory for Laser Energetics (LLE) and consultation with the Naval Research Laboratory (NRL). The facility utilizes symmetrically-illuminated targets and is designed to duplicate the anticipated time dependent radiation damage unique to ICF systems, in order to provide the technology base needed for an ICF demonstration facility. In the first year (1985) the study focused on cavity design and first wall protection, test module design and test coupon damage rate estimation, as well as placement and damage to the final mirrors.[1] In 1986, the effort was devoted to resolving some of the issues identified in the previous year and included a cavity design optimization and stress analysis, a blanket test module design and test program, a materials testing schedule, shield design, radioactivity and analysis and a cost estimate.[2]

In FY 86-87 the four tasks which were addressed are:

1. Impact of tritium breeding and self-sufficiency on the design and economics of SIRIUS-M.
2. Development of the beam crossover shielding concept.
3. Cavity design optimization with enhanced target performance.
4. Economic scaling of SIRIUS-M to a demonstration (DEMO) reactor facility.

A summary of the findings for each of the tasks listed above follows.

1. Impact of tritium breeding and self-sufficiency on the design and economics of SIRIUS-M.

The aim of this analysis is to determine if T_2 self-sufficiency can be achieved without compromising the primary mission of the reactor, namely to test materials for use in fusion power reactors.

Nine options using variations in materials, material composition, dimensions and design were investigated to determine the impact on the T_2 breeding ratio (TBR) and the displacement per atom (dpa) which is the measure of damage in the test samples within the materials test module. The dpa in the non-breeding base case will be taken as unity and the various options will be normalized to that for comparison. In the first four options, the water coolant was modified by the addition of $LiNO_3$ at a concentration of 20 g/100 cc. Further, the coolant fraction in the steel zone was increased from 10-20% and 10 cm of the Pb multiplier zone was traded for the steel reflector. This resulted in a TBR of 0.792 while the dpa was reduced by 2.7%. In the fifth option, the graphite tiles were replaced with Be tiles, boosting TBR to 0.85 with virtually no loss in dpa. We also tried increasing the $LiNO_3$ concentration to 80 g/100 cc. Although the TBR rose to 1.08, the probability of higher corrosion at this concentration did not allow us to favor this option. In the last two options the Pb was replaced with Be and the thickness of the multiplier/steel zones was varied holding the sum of the two constant. A TBR of 1.4 is achieved with almost no loss of dpa as compared to the Pb multiplier case with the same dimensions.

Table ES-1 gives a cost comparison between the base case without breeding and with breeding. Minor differences in design account for slight variation in the direct costs and total overnight costs. The total lifetime cost shows a decrease of 433 M$ for the breeding case, a 27% reduction over the non-breeding case. From the standpoint of radiation damage, the figure of merit given by M$/dpa shows a reduction of only 8%.

We conclude that T_2 self-sufficiency can be achieved by the simple addition of $LiNO_3$ to the cooling water and utilizing a front multiplier zone of either Pb or Be. A substantial savings over the lifetime costs can be realized by making the design T_2 self-sufficient.

2. Development of the beam crossover shield concept.

We have determined that a crossover in the laser beams is needed to reduce damage to the vacuum windows and limit neutron streaming through the beam tubes. Gas breakdown can occur at the focal point with attendant beam quality degradation.

For xenon gas at 1.0 torr and a KrF laser (0.25 μm), we estimate that the threshold for multiphoton absorption or tunneling occurs at 2×10^{13} W/cm^2 and cascade breakdown at 2.5×10^{15} W/cm^2. SIRIUS-M, using a 1.0 MJ laser, 10 ns pulse and 92 beams, if focused on a 1.0 cm diameter spot will have an energy density of 10^{13} W/cm^2. Based on this preliminary determination we would not expect breakdown to occur.

Increasing the number of beams to 92 and reducing the focal aperture from 10 cm to 2 cm reduces the dose to the window by 25 fold, with an end of life dose of 0.01 Mrad.

Table ES-1

Comparison of Costs for 13.4 MJ Target With and Without Breeding

Costs	1986 Base Case 13.4 MJ, 10 Hz 2 m Radius w/o Breeding	1987 Base Case 13.4 MJ, 10 Hz 2 m Radius w/Breeding
Bare Direct Costs (M$)	452	443
Total Overnight Costs (M$)	855	838
Operation & Maintenance (M$)	25.5	25
Fuel	36.3	-4.8*
Electric	13.2	13.2
Total Lifetime Cost (M$)	1605	1172
Figure of Merit (M$/dpa)	13	12

*Negative sign indicates credit for sold T_2.

3. Cavity design optimization with enhanced target performance.

It has been suggested that we consider a target with a yield of 100 MJ instead of the original 13.4 MJ for the SIRIUS-M reactor.

Calculating the surface heat flux from a 100 MJ target, the thermal response using graphite tiles and the thermal stress, we have determined that the cavity radius must be 4 m.

Table ES-2 compares the costs of using a 13.4 MJ target to a 100 MJ target, holding the neutron wall loading constant and assuming T_2 breeding in both cases. Credit is taken for excess T_2 at a price of \$10 x 10^3/g assuming there is a market for it. The bare direct costs and overnight costs are higher by 21% for the 100 MJ case but the lifetime costs are only 2.6% higher (due to the higher T_2 credit). The figure of merit in M\$/dpa increases from 12-12.3.

We therefore conclude that there is no incentive to use a more advanced higher yield target in SIRIUS-M.

4. Economic Scaling of SIRIUS-M to a DEMO reactor facility.

In our analysis we have assumed two ways of going to a DEMO reactor:

1. Design a so-called "Greenfield" DEMO. This means that a DEMO facility is started from ground zero.
2. Use the 100 MJ, 10 Hz, 4 m ETR SIRIUS-M facility and upgrade it to a DEMO. This would mean replacing the cavity, renovating the laser system power supply and optics. We assume it already has electric conversion and heat rejection equipment.

Table ES-2

Comparison of Costs for 13.4 MJ Target with Breeding and 100 MJ Target with Breeding

Costs	1987 Base Case 13.4 MJ, 10 Hz 2 m Radius w/Breeding	1987 100 MJ, 5.4 Hz 4 m Radius Constant r w/Breeding
Bare Direct Costs (M$)	443	538
Total Overnight Costs (M$)	838	1018
Operation & Maintenance (M$)	25	30.5
Fuel	-4.8*	-19.2*
Electric	13.2	7.1
Total Lifetime Cost (M$)	1172	1202
Figure of Merit (M$/dpa)	12	12.3

*Negative sign indicates credit for sold T_2.

Tables ES-3a and ES-3b give the costs of a 1370 MW_{th} "Greenfield" DEMO in 1986$. Total overnight costs are 1489 M$, total lifetime costs are 2383 M$, operation and maintenance is 44.7 M$/year and the levelized cost of electricity (COE) is 19 mills/kWh. Table ES-4 shows the case of upgrading a SIRIUS-M facility to a DEMO. Here we assume a new 4 m radius cavity will be needed and a 100 MJ target yield at 10 Hz will be used. Items that can be reused are indicated and the cost of additional equipment is tabulated. It shows that additional expenditures amount to 313 M$.

The conclusion is that a substantial saving of up to almost a B$ can be realized by upgrading a SIRIUS-M facility into a DEMO over a "Greenfield" DEMO.

Figure ES-1 is a cross section of the SIRIUS-M reactor building using 92 uniformly distributed beams. As has already been mentioned, the group at LLE has indicated that 32 beams provide marginal uniformity for symmetric illumination and that 96 beams are much more desirable. Since beam location and distribution have a direct impact on the design of the cavity and blanket, it is important to insure that the beam distribution is consistent with a reasonable blanket geometric configuration and amenable to remote maintenenace. We have found a configuration with 92 beams which satisfies these requirements. The spherical cavity is divided into 80 hexagonal and 12 pentagonal modules, with a beam port in the center of each one. The modules fit into a frame consisting of wedge shaped elements which interconnect the cavity. Modules can be removed from the cavity by simply disconnecting coolant lines and extracting them from the outside. An analysis of this configuration will be one of the tasks proposed for FY 88.

Table ES-3a

Bare Direct Capital Costs - SIRIUS-D (1000 MWth)

ITEM	M$
Land	0
Structures & Site Facilities	86
Reactor Plant	270
Turbine Plant	97
Electrical Plant	81
Miscellaneous Plant	32
Heat Rejection	21
Laser Driver (1 MJ)	100
Target Factory	100

Table ES-3b

Summary of "Greenfield" Costs for SIRIUS-D (1986$)

Capital Costs - $M	
Bare Direct Costs	787
Total Direct Costs	904
Total Overnight Costs	1489
Total Capital Costs	1930
Annual Costs - $M/y	
O & M	44.7
Fuel	0
Investment return	138
Total Lifetime Costs	2383
COE - Levelized	
Mills/kWh (with investment return)	76
Mills/kWh (without investment return)	19

Table ES-4

Build SIRIUS-D on SIRIUS-M Site

- Assume 4 m, 100 MJ, 10 Hz SIRIUS-M
- Items to be Reused
  - Building
  - Heat Rejection
  - Electric Plant
  - Turbine Plant
  - Miscellaneous Plant
  - Parts of Laser Excluding Optics
  - Target Factory
  - Instrumentaion and Control
  - Maintenance Equipment
  - Fuel Handling, Vacuum, Pellet Injection
  - Auxiliary Water Cooling
- Items to be Replaced or Added

	BDC-$M
Reactor Cavity	140
Laser Power Supply	32
Laser Optics	33
Breeding Equipment*	5
Heat Transfer Equipment*	103
	313

*Only if DEMO will have a liquid metal blanket

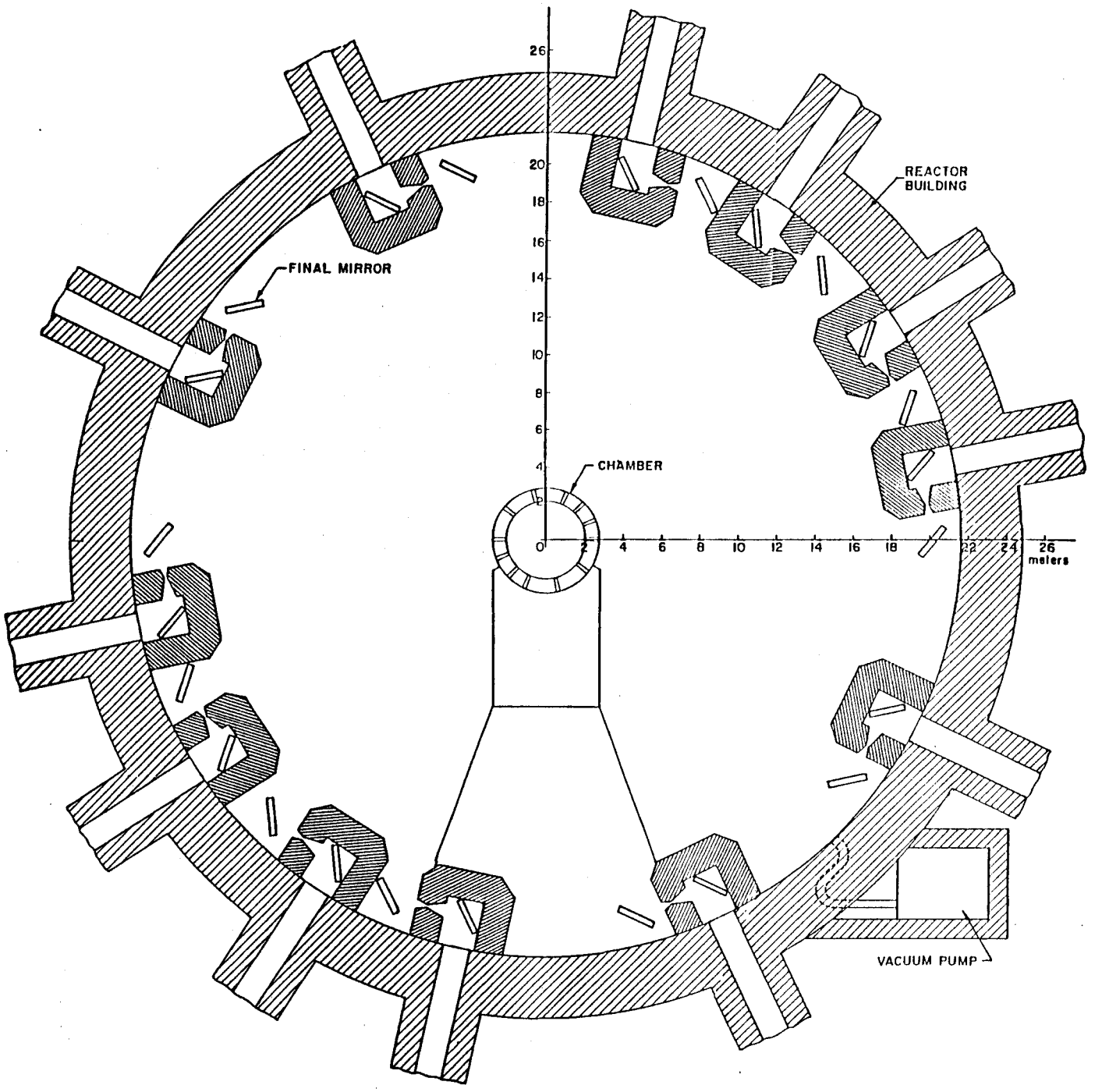

Fig. ES-1. Cross section of the SIRIUS-M reactor building using 92 uniformly distributed beam.

References for Executive Summary

1. B. Badger et al., "SIRIUS-M: A Symmetric Illumination, Inertially Confined, Direct Drive Materials Test Facility," University of Wisconsin Fusion Technology Institute Report UWFDM-651 (September 1985).

2. B. Badger et al., "SIRIUS-M: A Symmetric Illumination, Inertially Confined Direct Drive Materials Test Facility," University of Wisconsin Fusion Technology Institute Report UWFDM-711 (October 1986).

1. INTRODUCTION

It has long been known that the 14.5 MeV neutron generated by a DT fusion reaction will cause damage in structural materials which is vastly different from the much lower energy fission neutron. Clearly, structural materials must be tested and completely qualified before a DEMO fusion reactor can be contemplated. Irradiation of small material samples in a neutron flux can be performed in existing fission reactors or small DT neutron sources such as the RTNS.[1] However, the restricted temperature range and small test volumes, as well as serious neutron energy spectral differences, make complete testing of materials under realistic simulated conditions virtually impossible.

In the MFE (Magnetic Fusion Energy) program this issue has been addressed in several reactor studies both in the U.S. and in other countries (FERF, TETR, INTOR, TASKA, TDF and FEF). The ICF (Inertial Confinement Fusion) program, however, has had only one brief scoping study called LA FERF[2] performed at LLNL in 1975. There are major differences between the damage conditions in ICF and MFE, mainly due to geometric, spectral and temporal effects. The neutron spectrum incident on the first wall is no longer a simple gaussian about 14.1 MeV and considerable downgrading in the pellet can cause a very different response in the first wall. Further, the time over which the damage is produced varies from a few hundred nanoseconds for neutrons to 1-10 microseconds for the charged particles which are the pellet debris, and photons are essentially decoupled from the instantaneous damage caused by the neutrons and charged particles. Finally, the use of a low pressure gas in the chamber can significantly alter the energy spectra and flux to the first wall. All this points to the need for the development of a dedicated ICF materials test facility. To this end, beginning in 1985, the

Fusion Technology Institute of the University of Wisconsin (FTI) and the University of Rochester's Laboratory for Laser Energetics (LLE), in cooperation with the Naval Research Laboratory (NRL), initiated a study of the critical issues related to the design of an ICF materials test facility, SIRIUS-M. The facility uses symmetrically-illuminated targets and is designed to duplicate the time-dependent radiation damage structure unique to ICF systems, in order to provide the technology base necessary for an ICF demonstration facility. The results obtained during the first year of the study (1985) are given in Reference 3 and those obtained during 1986 in Reference 4. This report summarizes the results obtained by the FTI and LLE team related to the SIRIUS-M design effort during 1987.

During the first year of the study (1985), attention was focused on several areas unique to an ICF materials test facility including: test module design and damage rates estimation; cavity design and first wall protection; target design; placement and damage to the final mirrors. The work performed during the second year (1986) builds on the knowledge gained in these areas. Efforts have been devoted to resolving the critical issues identified in the first year. These included: a cost estimate, cavity design optimization, stress analysis, materials testing schedule, identification and testing of unique ICF blanket problems, shield design and radioactivity.

In 1987 the effort has been devoted to four primary tasks:

1. Impact of T_2 breeding and self-sufficiency on the design and economics of SIRIUS-M.
2. Development of a beam crossover shielding concept.
3. Cavity design optimization with enhanced target performance.
4. Economic scaling of SIRIUS-M to a DEMO reactor.

The report is organized in the following way. Chapter 2 deals with the economic analysis of T_2 self-sufficiency. In Section 2.1 we describe a detailed trade study of the various options considered to enhance T_2 breeding while retaining the primary product of the reactor, namely material radiation damage in the material test modules. Section 2.2 examines the economic impact of T_2 breeding on the base case. These two aspects are quantified in the amount of dollars saved over the lifetime of the reactor and the reduction in damage given by the figure of merit M$/dpa.

Chapter 3 discusses the reactor shielding and building design. Here we summarize the various shielding options in Section 3.1 and discuss the beam crossover and its impact on the shielding in Section 3.2. The problem of gas breakdown at the beam focal point is also treated here. Finally the T_2 considerations are discussed in Section 3.3.

The impact of using a 100 MJ target on the cavity design, reactor performance and economics is the subject of Chapter 4. Section 4.1 covers the cavity gas response to the enhanced target, the first wall temperature response and the resultant thermal stresses. Section 4.2 discusses the economic impact.

In Chapter 5 we investigate the economic implication of scaling SIRIUS-M to a DEMO reactor. A set of design parameters consistent with the requirements of a DEMO reactor is selected in Section 5.1 and a bottoms up cost estimate is given in Section 5.2. Section 5.2.1 compares the cost of a so-called "Greenfield DEMO" with a "SIRIUS-M Upgrade DEMO." Here a "Greenfield DEMO" means a totally new facility, whereas in the upgrade version, much of the original equipment can be renovated and used again.

The summary and conclusions are given in Chapter 6.

References for Chapter 1

1. R.A. Van Konyneburg, H.H. Barschall, R. Booth and C. Wong, Proceedings of the Inter. Conf. on Radiation Test Facilities for CTR Surface and Materials Program, Argonne, IL, ANL/CTR-75-4, 171 (1975).

2. J. Hovingh, "Analysis of a Laser Initiated, Inertially-Confined Reactor for a Fusion Engineering Research Facility (LA FERF)," UCRL-76517, May 1975.

3. B. Badger et al., "SIRIUS-M: A Symmetric Illumination, Inertially Confined Direct Drive Materials Test Facility," University of Wisconsin Fusion Technology Institute Report UWFDM-651, September 1985.

4. B. Badger et al., "SIRIUS-M: A Symmetric Illumination, Inertially Confined Direct Drive Materials Test Facility," University of Wisconsin Fusion Technology Institute Report UWFDM-711, October 1986.

2. ECONOMIC ANALYSIS OF T_2 SELF-SUFFICIENCY

2.1 Potential for T_2 Self-Sufficiency in SIRIUS-M

The spherical SIRIUS-M chamber has an inner radius of 2 m with 2.5 cm thick protective tiles that consist of a 1 cm thick graphite layer and a 1.5 cm thick water-cooled structural support (40% PCA and 60% H_2O). In order to enhance the damage rate in the test modules, a 40 cm thick liquid lead self-cooled reflector (90% liquid Pb and 10% PCA) is utilized behind the graphite tiles. The primary support structure for the chamber is a 30 cm thick water-cooled stainless steel reflector (90% PCA and 10% H_2O) that follows immediately behind the lead reflector. In this design, tritium breeding and high temperature recovery of thermonuclear energy were excluded in order to simplify the design of this first-of-a-kind facility and reduce its capital cost. The SIRIUS-M facility consumes tritium at the rate of ~ 3.4 kg/year with the tritium cost representing nearly 50% of the annual operating cost.[1] This motivated us to investigate the impact of tritium breeding and self-sufficiency on the design and economics of SIRIUS-M.

Modifying the chamber design to breed as much tritium as possible without compromising design simplicity was considered. An attractive concept that meets this requirement is the aqueous self-cooled blanket concept[2] where small amounts of lithium compounds are dissolved in the water coolant. This preserves the attractive features of low pressure low temperature blankets. Many Li compounds have high solubility limits in water allowing for significant tritium breeding. The choice of the Li salt depends on several considerations that include tritium breeding potential, compatibility with structural materials, induced radioactivity and salt radiolysis. $LiNO_3$ was chosen for the baseline design of the breeding shield in the TIBER-II tokamak test

reactor[3] and will be used in SIRIUS-M. The solubility limit for $LiNO_3$ in cold water is 89.8 g/100 cm^3. Provided that tritium breeding is adequate, the lower salt concentration is preferable due to reduced corrosion rate and activation products.

Several one-dimensional neutronics calculations were performed to determine the impact of blanket design on achievable overall tritium breeding ratio (TBR) and damage rate in test modules. The discrete ordinates code ONEDANT[4] was used with cross section data based on the ENDF/B-V[5] evaluation. The reactor was modeled in spherical geometry with a point source at the origin emitting neutrons with energy distribution given by the SIRIUS-M target spectrum. Following neutron interactions with target materials 1.053 neutrons are emitted from the target per DT fusion.

The overall TBR was calculated taking into consideration that the beam penetrations occupy 2% of the inner blanket surface and the test modules cover 4% of the area. While only 2% of the source neutrons stream directly through the beam ports and do not contribute to tritium breeding, some of the neutrons reentering the cavity after diffusing in the blanket might stream through the beam ports yielding further reduction in TBR. Meier[6] performed three-dimensional neutronics calculations for a spherical chamber with two diametrically opposed beam ports for Li and $Li_{17}Pb_{83}$ blankets. The results indicated that the TBR decreases at a rate greater than predicted based on the loss of blanket coverage. Eight and twenty percent reduction in TBR was obtained for Li and $Li_{17}Pb_{83}$, respectively, for ports subtending 5% of the total solid angle. Careful examination of the results indicates that the larger streaming neutron fraction and the enhanced reduction in TBR are related to the number of neutrons reentering the cavity.

We derived the following analytical expression for the drop in the number of neutrons incident on the blanket in SIRIUS-M relative to the number incident on a full coverage blanket:

$$\frac{\Delta n_B}{n_B} = \frac{1 - C_B - r_{TM}\, C_{TM}}{1 - (r_B C_B + r_{TM} C_{TM})} \,. \tag{1}$$

C_B and C_{TM} are the coverage fractions of the blanket and test modules, respectively. r_B and r_{TM} are the average neutron reflectivities of the blanket and test module, respectively. The average reflectivity (r) is determined from the number of neutrons reentering the cavity per source neutron (R) via

$$R = r + r^2 + r^3 + \ldots = \frac{r}{1-r} \,. \tag{2}$$

For each blanket design, in addition to calculating the full coverage TBR, the number of reentering neutrons was determined from the one-dimensional calculation. It was then assumed that the fractional drop in TBR will be the same as the fractional drop in the number of neutrons incident on the blanket as given by Eq. (1). Although this calculational procedure assumes that the same number of neutrons are reflected per incident neutron regardless of its energy spectrum, it gave nearly identical values for the number of neutrons streaming through the penetrations and conservatively lower estimates for the overall TBR when compared to the three-dimensional results of Meier. Using Eqs. (1) and (2) is expected to yield an even more conservative estimate for the overall TBR in SIRIUS-M where a large number of small beam ports are used leading to a larger chance for the streaming neutrons to enter the blanket from the

penetration walls and contribute to breeding. In SIRIUS-M, the values used for C_B, C_{TM} and r_{TM} in Eq. (1) are 0.94, 0.04, and 0.777, respectively.

The impact of the blanket design on the peak dpa rate achievable in the test modules was determined by calculating the dpa rate in iron using the neutron flux at the inner surface of the blanket obtained from the one-dimensional calculation. Calculations were also performed for the nonbreeding chamber design and the results used as a basis for comparing the testing capability of the device with the different breeding blanket design options.

The results of the calculations performed for different blanket design options are tabulated in Table 2.1-1. Option 1 corresponds to the nonbreeding chamber design with a self-cooled liquid lead reflector. In the breeding design options $LiNO_3$ is dissolved in the water coolant. Concentrations of 20 and 80 g/100 cm^3 were considered. Because of the soft neutron spectrum in the blanket resulting from using neutron multipliers, lithium in the aqueous solution is enriched to 90% ^6Li. Options 2 and 3 represent the least modification to the nonbreeding design with the Li compound added to the water coolant for the tile and steel reflector. It is clear that no tritium self-sufficiency can be achieved in these designs even with the large Li compound concentration (option 2). It was observed that ~ 70% of tritium breeding occurs in the coolant for the tiles. This motivated us to increase the aqueous solution content in the steel zone to 20% in options 4 and 5 that resulted in ~ 15% increase in the TBR with tritium self-sufficiency being possible when a $LiNO_3$ concentration of 80 g/100 cm^3 is used. As indicated earlier in this section, using low salt concentration is preferable to reduce corrosion and activation products. The other design options considered here are aimed at modifying the blanket design to achieve tritium self-sufficiency with a $LiNO_3$ concentration of 20 g/100 cm^3 of the coolant.

Table 2.1-1

Impact of Blanket Design on TBR and Testing Capability

Option	Tile Material	Multiplier Material	Multiplier Zone Thickness (cm)	Steel Zone Thickness (cm)	% H_2O in Steel Zone	$LiNO_3$ Concentration (g/100 cm^3)	Overall TBR	Relative dpa Rate in Test Module
1	C	Liquid Pb	40	30	10	0	0	1
2	C	Liquid Pb	40	30	10	80	0.942	0.982
3	C	Liquid Pb	40	30	10	20	0.668	0.991
4	C	Liquid Pb	40	30	20	80	1.055	0.982
5	C	Liquid Pb	40	30	20	20	0.786	0.991
6	C	Liquid Pb	30	40	20	20	0.792	0.973
7	Be	Liquid Pb	30	40	20	20	0.850	0.991
8	C	Solid Pb	30	40	20	20	1.132	0.795
9	C	Be	15	55	20	20	1.077	0.787
10	C	Be	30	40	20	20	1.399	0.790

In design option 6, the front multiplier zone thickness is decreased by 10 cm while the steel reflector thickness is increased by 10 cm. This results in increasing the TBR by less than 1%. The effect of replacing the graphite tiles by beryllium tiles can be assessed by comparing the results for options 6 and 7. The TBR increases by ~ 7% and the damage rate in the test modules increases by ~ 2% due to the increased neutron multiplication. Although using Be tiles is beneficial from the neutronics point of view other design considerations related to the excessive temperatures obtained and physical properties of Be lead to discarding this option. In option 8, tritium breeding is achieved in the multiplier zone by using solid lead cooled by the aqueous solution instead of the self-cooled liquid lead. The multiplier zone consists of 70% Pb, 10% PCA and 20% aqueous solution. Tritium self-sufficiency can be achieved using this blanket design. However, due to the increased neutron absorption in the Li used in the front multiplier zone, the damage rate in the test module is ~ 20% lower than that obtained in the nonbreeding chamber design (option 1). Replacing the Pb by Be in the multiplier zone results in higher TBR with T_2 self-sufficiency being achievable with a thinner multiplier zone as indicated in option 9. It should be noted that the results in Table 2.1-1 do not account for tritium breeding in the blanket zones behind the 20 cm thick test modules which can increase the tritium breeding margin. Adding the contribution from these zones was found to increase the overall TBR by ~ 2%.

We conclude from the results of Table 2.1-1 that tritium self-sufficiency can be achieved in SIRIUS-M by adding $LiNO_3$ to the water coolant with a front multiplier zone utilizing Pb or Be. Using a self-cooled liquid lead blanket, tritium self-sufficiency can be achieved only if a high concentration of $LiNO_3$

close to its solubility limit is used. This option has the advantage of having a negligible impact (< 2%) on testing capability of the device. On the other hand, the high salt concentration can lead to excessive corrosion and activation products. In addition the heavy weight of lead and the potential problem of polonium production are of concern for this design option. Alternatively, using solid lead cooled by the aqueous solution allows for tritium self-sufficiency with a relatively low salt concentration (20 g/100 cm^3). However, in this case, ~ 20% degradation in testing capability occurs. This design option still suffers from the problems associated with using lead such as heavy weight, low strength, large creep, low modulus, high stress cracking in water, low melting point, and Po production. Using Be multiplier results in tritium self-sufficiency with only 15 cm thick multiplier zone and 20 g $LiNO_3$ per 100 cm^3 of the coolant. Be has the advantage of being light and more compatible with the aqueous solution than Pb. However, as in the case of solid Pb, the testing capability of the facility is degraded by ~ 20% compared to the nonbreeding chamber design. The blanket design with Be multiplier is considered as the baseline design for the tritium breeding blanket design in SIRIUS-M. Using Be as neutron multiplier has the potential for achieving a TBR much greater than unity as indicated in design option 10. In this case, in addition to utilizing SIRIUS-M for ICF technology testing, it can be used as a tritium production facility.

2.2 Economic Impact of T_2 Breeding for Base Case

In this section we will compare the costs and the figure of merit (FOM), of the original base case (13.4 MJ, 2 m) and the base case with T_2 breeding included.

Figure 2.2-1 shows a representative geometry for the 2 m 13.4 MJ cavity. The first wall made of graphite tiles is at 2 m from the target. Its thickness is 1 cm and is followed by 1.5 cm of cooling channels. Next comes the zone containing the neutron multiplier and/or T_2 breeding material. The final zone again contains the steel structure and cooling channels. The thicknesses of the last two zones vary in such a manner that the final radius of the reactor stays constant at 270 cm. The breeding material can be either 90% enriched $LiNO_3$ dissolved in the cooling water (in all three zones) or LiPb that replaces water in zone 3 (multiplier zone). The $LiNO_3$ concentrations in water are either 20 g/100 cc or 80 g/100 cc of water. The base case (no breeding) had liquid lead in zone 3 (40 cm) followed by 30 cm of steel and water. In the breeding scenarios, the multiplier is either Be balls, or lead (solid or liquid). Be in the third zone tends to decrease the damage rate in the test modules by 15-20% due to forwardly peaked scattering of neutrons and a softer neutron spectrum. In addition, if there is breeding material in that zone, the neutrons are absorbed in Li.

The 6 representative breeding configurations for the 2 m, 13.4 MJ cavity are shown in Tables 2.2-1 and 2.2-2. In Table 2.2-1, the cases are identified and related to applicable cases in Table 2.1-1. Presented are the total tritium breeding ratio (TBR), energy multiplication and loss in the damage rate in the test sample due to the effects discussed above. Also presented are the adjustments in the direct cost of the reactor chamber that need to be made over the base case. These adjustments are due to the cost of additional materials ($LiNO_3$, Be, LiPb, PCA) and displaced materials (Pb, PCA). In Table 2.2-2 the adjustments are combined to give the total difference in cost of the

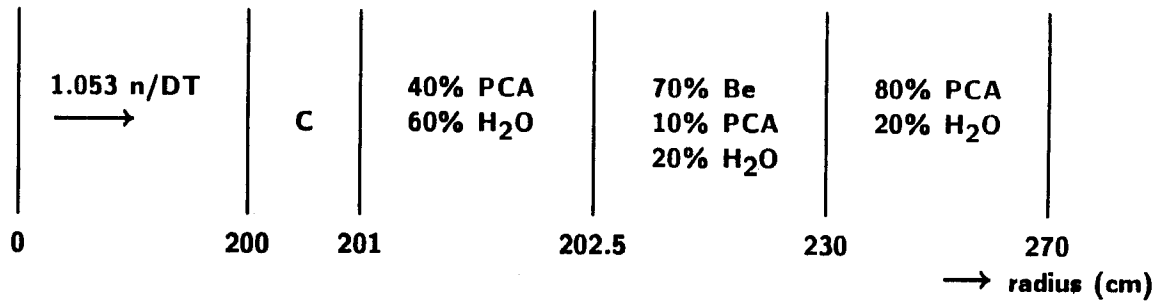

Fig. 2.2-1. Representative case of a 2 m SIRIUS-M cavity with T_2 breeding, showing compositions and thicknesses of various zones. Not drawn to scale.

Table 2.2-1. 2 m Cases With Breeding

	Case	Applicable Option Number from Table 2.1-1	Fuel Revenue ($M)	TBR	Energy Multiplication	Dpa Loss (%) (total dpa-ℓ)	Cost of $LiNO_3$ ($M)	Cost of Be ($M)	Cost of LiPb ($M)	Cost of Pb ($M)	Cost of PCA
ΔBe, 30 cm 20 g/100 cc $LiNO_3$	1	10	14.44	1.399	1.33	20.9 (11,232)	0.62	9.43	0	-1.25	-0.33
ΔBe, 15 cm, 20 g/100 cc $LiNO_3$	2	9	2.75	1.077	1.30	21.3 (11,175)	0.62	3.99	0	-1.25	-0.33
30 cm, liq. Pb, 80 g/100 cc $LiNO_3$	3	NA	2.79	1.077	1.35	3.6 (13,689)	0.81	0	0	-0.35	+0.28
30 cm, solid Pb, 20 g/100 cc $LiNO_3$	4	8	4.78	1.132	1.35	20.5 (11,289)	0.62	0	0	-0.62	-0.33
Be + LiPb, no salt, 25 cm	5	NA	5.57	1.154	1.38	15.6 (11.985)	0	7.54	1.06	-1.25	-0.33
Be + LiPb, no salt, 30 cm	6	NA	10.72	1.296	1.37	15.6 (11,985)	0	9.43	1.32	-1.25	-0.33

Table 2.2-2

Case	Reactor Cavity, ΔC ($M)	Breeding Equipment, ΔC ($M)	HT eq't, ΔC ($M)	Total, ΔC	Fuel Credit
1	8.47	7.2	-15.9	-0.2	14.44
2	3.03	7.2	-16.2	-6.0	2.75
3	0.74	7.2	-4.9	+3.0	2.79
4	-0.33	7.2	-15.6	-8.7	4.78
5	7.02	7.2	-6.7	+7.5	5.57
6	9.17	7.2	-4.9	+11.5	10.72

reactor cavity. Cost of additional breeding equipment is also shown ($2.2 M for isotope separation, TSTA figures,[7,8] $5 M for extraction of T_2 from breeding material). Adjustments in the cost of the heat transfer equipment need also be made because we are replacing expensive liquid metal cooling by water cooling to a varying degree. (There are also slight differences in energy multiplication.) This information yields the total difference in direct cost which can be either positive or negative. For case 1, Be balls in zone 3 with 20 g/100 cc dissolved $LiNO_3$, this total cost difference is almost zero. The huge negative difference caused by replacing all of liquid lead cooling by water cooling is offset by putting a lot of expensive Be in the reactor chamber. This case also has the highest fuel credit due to the high TBR of 1.399 (shown in last column and assuming that T_2 price of $10,000/g can be maintained). Case 4 has the lowest direct cost, because the lower cost of H_2O cooling is not offset by an increase in reactor cavity cost (there is no Be and $LiNO_3$ cost is offset by a decrease in the cost of Pb and PCA displaced). This case has a medium fuel credit. Case 6 has the highest net gain in direct cost (most of liquid Pb cooling is replaced by LiPb cooling which costs the same, only a fraction is replaced by cheaper water cooling). The increase in reactor cavity cost is high due to the cost of Be and 90% enriched LiPb. This case has a relatively high fuel credit, too. Similar calculations were done for these 3 cases for the 100 MJ, 4 m design.

The 13.4 MJ designs with T_2 breeding can be compared as to their total overnight cost (TOC), annual costs, total lifetime costs and figures of merits (FOM). The total lifetime cost is defined as the sum of TOC and the annual costs summed over the life of the facility. The annual costs incorporate operation and maintenance costs (cost of personnel, equipment and non-fuel

materials to run the plant), fuel costs and electricity costs (mainly for laser input power). The O&M costs are taken as a fraction of the TOC. The fuel costs are negative in case of T_2 breeding and the fuel credit is assumed to be based on the prevailing purchasing price of T_2 ($10,000/g), other fuel costs and losses being neglected. Other cases for the fuel cost are considered in Section 4.2 in which both the 13.4 MJ and enhanced target designs are compared with respect to economic considerations. The electricity costs for the laser power supply are assumed to be 3¢/kWh (other power users are neglected); other electricity cost options and other drivers for SIRIUS-M are considered in more detail elsewhere.[9] The option of producing part or all of the electricity required from the reactor fusion power is discussed in 5.2.1.

The FOM is defined as the ratio of total lifetime cost and the cumulative induced damage in the test modules (in dpa-ℓ). An alternative figure of merit, FOM_1, which more truly reflects the cost of borrowed money under the assumptions used[9] can also be used. This figure of merit is given by:

$$FOM_2 = 0.277\ BDC + AC$$

where BDC is the bare direct cost of one facility (i.e. installed cost of equipment assuming instantaneous installation, and excluding indirect costs and contingencies)[9] and AC is the total annual cost described above. This FOM doesn't incorporate the cumulative damage, because a certain minimum wall loading ($\sim 2\ MW/m^2$) is required and damage rate (in dpa/yr) is proportional to the wall loading. Based on the original FOM, the best 2 m configuration is the one with the liquid Pb zone with H_2O shield and first wall cooling

containing 80 g/100 cc $LiNO_3$ (Case 3 in Table 2.2-1). If FOM_1 is used as the discriminator, then the best 2 m case is the one with the 30 cm Be zone and H_2O cooling with 20 g/100 cc of dissolved $LiNO_3$.

If no fuel credit is allowed for bred T_2, and if a minimum wall loading of ~ 2 MW/m^2 is required, then by far the best case has the 30 cm solid Pb multiplier zone cooled by H_2O with 20 g/100 cc dissolved $LiNO_3$ as the breeder. If there is no market for bred T_2, then the object is to reduce the amount of T_2 produced and the best case is the design with a 30 cm liquid lead zone and H_2O cooling elsewhere with 80 g/100 cc dissolved $LiNO_3$. However, in that case the price of T_2 purchased would probably be low, and if we don't want to introduce any additional T_2 into the economy, then the base case (2 m, 10 Hz, 13.2 MJ) without breeding is the only case to be considered.

The above design options for the 2 m, 13.4 MJ, 10 Hz facility are shown in Tables 4.2-3 and 4.2-4 along with the representative cases for the enhanced target ETR (100 MJ and 4 m cavity). These cases are given more consideration in 4.2 where the base case and enhanced target design options are compared.

References for Chapter 2

1. B. Badger et al., "SIRIUS-M: A Symmetric Illumination, Inertially Confined Direct Drive Materials Test Facility," UWFDM-711, University of Wisconsin (1986).

2. D. Steiner et al., "Application of the Aqueous Self-Cooled Blanket Concept to Fusion Reactors," Trans. Am. Nucl. Soc., 52, 129 (1985).

3. M. Sawan, "Potential for Tritium Breeding in the Compact Tokamak Test Reactor TIBER-II," Trans. Am. Nucl. Soc., 54, 120 (1987).

4. R. O'Dell et al., "User's Manual for ONEDANT: A Code Package for One-Dimensional, Diffusion-Accelerated, Neutral-Particle Transport," LA-9184-M, Los Alamos National Lab. (1982).

5. D. Garber, "ENDF/B-V," BNL-17541 (ENDF-201), National Nuclear Data Center, Brookhaven National Lab. (1975).

6. W. Meier, "Neutron Leakage Through Fusion Chamber Ports: A Comparison of Lithium and Lead-Lithium Blankets," Nucl. Tech./Fusion, 3, 385 (1983).

7. Private communication from James L. Anderson, Tritium Systems Test Assembly, Los Alamos National Laboratory.

8. John R. Bartlit, James L. Anderson, V.G. Rexroth, "Subsystems Cost Data for the Tritium Systems Test Assembly," in the IEEE Proceedings of the 10th Symposium on Fusion Energy, Philadelphia, PA, Dec. 5-9, 1983.

9. Zoran Musicki, "The Economic Analysis of SIRIUS-M, A Symmetrically Illuminated Inertial Confinement Fusion Engineering Test Reactor," UWFDM-708, September 1986.

3. SHIELD AND BUILDING DESIGN

3.1 Summary of Design Options

In laser driven fusion reactors neutrons emitted from the target stream directly into the beam ducts producing significant damage in optical windows and final mirrors. Previous analyses for SOLASE[1] and SENRI-I[2] indicated excessive streaming into the laser building. While penetration shielding space is not at a premium in these double-sided target illumination designs, designing the penetration shield and building for reactors with symmetrically-illuminated targets, where a large number of beams ($\geq$ 32) is used, is of great concern. Three-dimensional neutronics calculations have been performed using the continuous energy Monte Carlo code MCNP[3] to analyze the different shield and building design options for SIRIUS-M.[4] The shield design criteria include: dose rate less than 2.5 mrem/hr outside the building during operation; minimum neutron streaming to the laser building during operation; and acceptable damage levels to optical windows and final mirrors.

Eight different shield and building design options were considered. The final mirrors are located 20 m from the target. In options I-IV, shown in Fig. 3.1-1, a 3 m thick concrete shield surrounds the reactor chamber. In option I, a 3 m thick concrete shield should surround the beam duct to reduce the dose outside the building to acceptable levels. The penetration shields for adjacent beam ducts will overlap with a large amount of concrete needed. In options II-IV, a single 1 m thick concrete building wall is used at a radius of 15 m. In option II, vacuum is maintained in all the space inside the building wall. In option III, a 1 cm thick aluminum pipe surrounds the laser beam and in option IV, borated water is utilized inside the building.

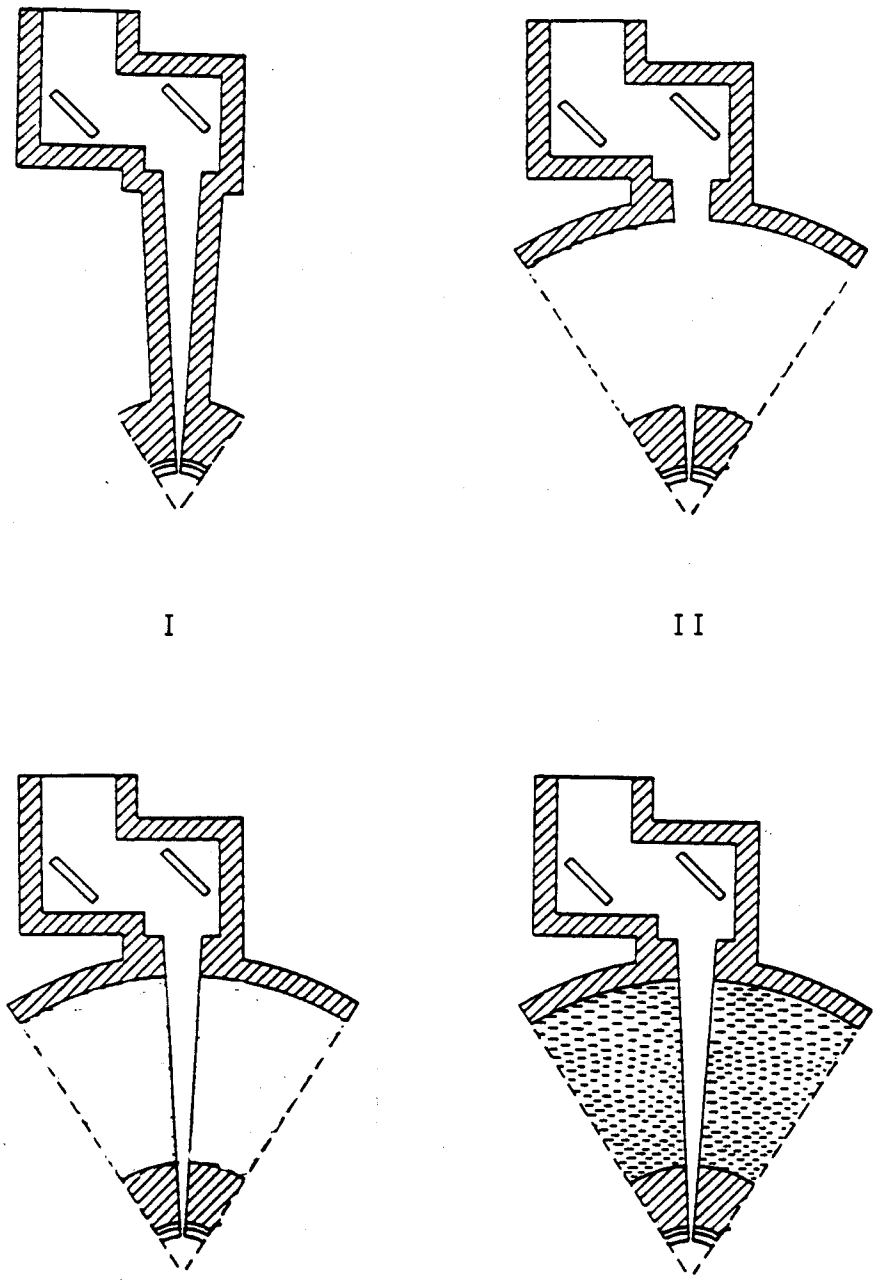

Fig. 3.1-1. Geometrical configurations for design options I-IV.

Radiation streaming into the final mirrors compartment necessitates surrounding these mirrors by concrete shield of at least 3 m thickness. The final mirrors enclosures will, therefore, overlap leading to an effective 10 m thick building wall with beam ducts and final mirrors embedded in it. We found that the goal dose rate of 2.5 mrem/hr outside the building during operation can be achieved with the least amount of shield if a 3.2 m thick concrete building wall is used behind the final mirrors as in options V-VIII, illustrated in Fig. 3.1-2. No concrete bulk shield surrounds the lead and steel reactor chamber in this case. While no shield encloses the final mirrors in option V, partial enclosures are used in options VI and VII. Option VIII requires beam point crossover optics[1] that allow surrounding the turning mirror by 1.5 m thick concrete shield with a 0.1 m diameter aperture. This approach was found to reduce streaming by ~ 3 orders of magnitude in SENRI-I.[2] In this design, possible filling gas breakdown is a concern with adequate vacuum needed in the aperture. In all eight design options, the shield is lined with a 1 cm thick layer of boral which reduced the streaming in SOLASE by an order of magnitude.

The peak radiation damage per full power year (FPY) and peak nuclear heating given in terms of absorbed dose rate are given in Table 3.1-1 for the eight design options analyzed. The results are nearly identical for options I-IV. The final focusing and turning mirrors suffer the largest damage in option V where no mirror enclosure is used. The damage in the turning mirror is extremely low in option VIII since it is almost fully enclosed by the shield. Based on preliminary data for ion irradiated coatings,[5] a limit of 2-3 x 10^{10} rads to the laser mirror coatings is desirable. The final focusing

Table 3.1-1

Neutron Streaming to Laser Building and Peak Radiation Effects in Final Mirrors and Laser Window

Option	Final Focusing Mirror		Turning Mirror		Neutrons Streaming per cm^2 of Laser Window for One Source Neutron	Dose Rate in SiO_2 Laser Window (rad/FPY)
	Al dpa/FPY	Rad/FPY	Al dpa/FPY	Rad/FPY		
I	0.0762	6.12×10^{10}	0.0011	9.72×10^{8}	3.65×10^{-11}	7.22×10^{7}
II	0.0741	6.03×10^{10}	0.0010	9.85×10^{8}	4.01×10^{-11}	7.93×10^{7}
III	0.0725	5.90×10^{10}	0.0009	7.88×10^{8}	3.98×10^{-11}	7.87×10^{7}
IV	0.0729	5.93×10^{10}	0.0011	7.58×10^{8}	3.55×10^{-11}	7.02×10^{7}
V	0.0980	8.52×10^{10}	0.0035	4.80×10^{9}	7.37×10^{-10}	1.33×10^{9}
VI	0.0967	8.17×10^{10}	0.0008	1.33×10^{9}	4.56×10^{-11}	8.13×10^{7}
VII	0.0777	6.32×10^{10}	0.0011	9.11×10^{8}	5.53×10^{-11}	1.02×10^{8}
VIII	0.0779	6.55×10^{10}	2.5×10^{-9}	1.17×10^{7}	2.50×10^{-14}	4.61×10^{4}

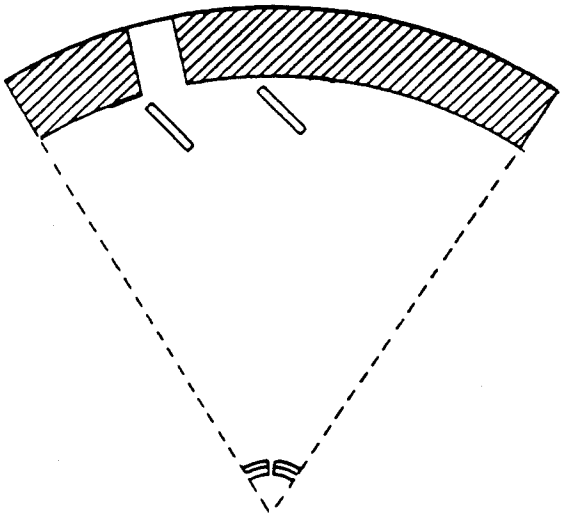

V

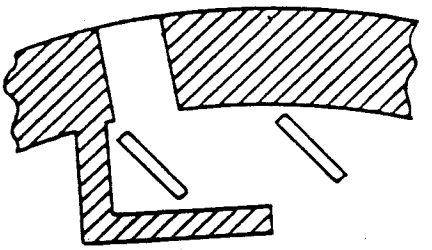

VI

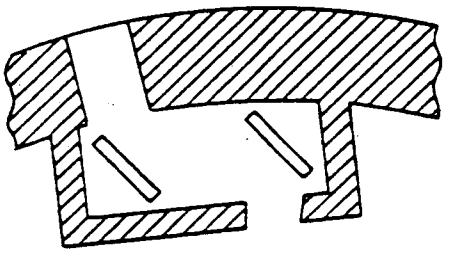

VII

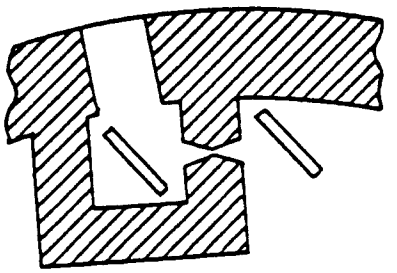

VIII

Fig. 3.1-2. Geometrical configurations for design options V-VIII.

mirror has to be replaced once or twice during a calendar year, while the final turning mirror should last the entire reactor lifetime. The number of neutrons streaming to the laser building per unit area of the laser window per source neutron as well as the dose rate in the SiO_2 laser window are given in Table 3.1-1. Design V results in the largest streaming and damage to the laser window. About three orders of magnitude reduction in streaming is obtained by adopting design option VIII. In this case, the absorbed dose in the laser window after the 5 FPY reactor life is 0.23 Mrad which is so low that the density decrease will be negligible (<< 0.01%) and very little optical degradation is expected.[5] Design option VIII, which meets all the design criteria, has been chosen as the base shield design for SIRIUS-M. However, its success depends on the viability of the beam crossover shielding concept discussed in the following section.

References for Section 3.1

1. M. Ragheb, A. Klein and C. Maynard, "Neutronics Shielding Analysis of the Laser Mirror-Beam Duct System for a Laser Fusion Power Reactor," Nucl. Tech./Fusion, 1, 99 (1981).

2. H. Oomura et al., "Radiation Streaming Analysis for the Beam Ports of the Laser Fusion Reactor, SENRI-I," Nucl. Tech./Fusion, 5/1, 80 (1984).

3. "MCNP - A General Monte Carlo Code for Neutron and Photon Transport," LA-7396-M, Los Alamos National Laboratory (1981).

4. S. Abdel-Khalik et al., "SIRIUS-M: A Symmetric Illumination, Inertially Confined Direct Drive Materials Test Facility," J. Nucl. Mat., 141-143, 1025 (1986).

5. G.L. Kulcinski, University of Wisconsin-Madison, personal communication (Sept. 1986).

3.2 Beam Crossover Considerations

Neutron streaming through beam ports has always been a matter of concern for ICF reactor designers, both from the standpoint of protecting optical elements and of minimizing the radiation dose at the reactor containment building boundary. The various options considered for reducing this neutron and γ streaming have been described in the previous section where a beam crossover has been identified as a major contributor to the reduction of streaming. A beam crossover is a point at which the laser beam is focused to a small area and then allowed to diverge again. The focal point requires a much smaller aperture than the beam itself and thus limits the number of neutrons that can pass through and progress further.

A possible problem that can arise at a crossover point is gas breakdown. Since the energy of the laser is concentrated at the focal point, the gas in the aperture can become ionized and lead to multiphoton absorption or tunneling and cascade breakdown which could degrade the quality of the laser beam. In the latest version of SIRIUS-M which has 92 beams, the 1.0 MJ laser using a 1.0 ns pulse will have a total power per beam of 10^{13} W and if focused to an area of 1.0 cm^2 will have a power density of 10^{13} W/cm^2. We estimate that for xenon gas at 1.0 torr pressure, in conjunction with a KrF laser which has a wavelength of 0.25 μm, the threshold for multiphoton absorption or so called tunneling occurs at 2×10^{13} W/cm^2. Cascade breakdown occurs at a much higher power density of 2.5×10^{15} W/cm^2. On this basis we do not expect breakdown to occur in the beam crossover points of the SIRIUS-M reactor using 92 beams.

It should be noted that the neutronics results given in Table 3.1-1 were calculated for SIRIUS-M with 32 beams. However, the results are still valid for the design with 92 beams as long as the final mirrors are kept at 20 m

from the target and the aperture diameter at the crossover point remains unchanged. The reason is that the neutron flux at the final mirrors and crossover point aperture is determined by the distance from the target and the target yield and is nearly independent of the number of beam penetrations. On the other hand, in the design which utilizes a beam crossover, the damage to the laser window scales with the aperture area. Reducing the aperture diameter from 10 cm to 2 cm brings down the dose rate in the SiO_2 laser window from 4.6×10^4 to 1.84×10^3 rad/FPY leading to an end-of-life dose of 0.009 Mrad, with negligible optical degradation expected.

3.3 Tritium Considerations

3.3.1 Introduction

A preliminary assessment is presented of the location and quantities of tritium and tritiated materials which may exist in the operational reactor building. The tritium resides in essentially two systems, namely: (1) the captive tritium contained in the fueling system and in the breeding blanket of the reactor shield, and (2) the tritium which exists in the gaseous atmosphere of the reactor building and some of which adsorbs onto the exposed surfaces in the building and in the reactor cavity. These systems are discussed and the potential release of tritium from these systems to the environment is assessed.

3.3.1.1 Tritium Inventory in the Fueling System and Breeder Blanket

The direct-illumination fuel target with 100 MJ of fusion power released will contain 0.65 mg T (Table 3.3-1) and 0.44 mg D. These targets will be prepared in a separate fuel assembly building and only a small inventory of targets will be on-hand in the reactor building. A 10 minute supply of targets would contain only 0.6 g of tritium and be safely contained in a heavy cryogenic refrigerator.

Table 3.3-1. Target Parameters for 100 MJ Yield

	Fuel Target	Target Debris
D	1.26×10^{20}	9.08×10^{19}
T	1.26×10^{20}	9.08×10^{19}
He	----	3.50×10^{19}
C	4.91×10^{19}	4.91×10^{19}
H	9.83×10^{19}	9.83×10^{19}

An additionally significant quantity of tritium would be contained in the aqueous breeder-coolant of the reactor shield, if it were decided to breed tritium on-site by this technique. The 4 m radius reactor cavity with a shield 40 cm thick, containing 20 vol.% water, would contain approximately 16 m^3 of aqueous breeder material. This aqueous solution would be continuously circulated during reactor operation for heat removal and a small side-stream would be diverted to the water detritiation facility. Experience at heavy-water cooled fission power plants has shown that there are only small radiation hazards to plant workers or the public for tritium concentrations in the water up to ~ 30 Ci/kg when the water is at low pressure and temperature.[1] On the other hand, a lower tritium concentration may be desirable in order to reduce the total tritium inventory and reduce the purchased amount of tritium required for startup of the facility. Because SIRIUS-M is a materials test reactor which will not operate continuously, a small-size water detritiation unit could continue to operate during the reactor downtime. A related study for the magnetic fusion experimental reactor,[1] TIBER-II, indicated that an average tritium concentration of ~ 5 Ci/kg would be cost-effective for such types of facilities; based on similar assumptions the SIRIUS-M reactor shield would contain 8 g of tritium in the aqueous coolant.

3.3.2 Tritium Inventory in the Reactor Building

A tritium inventory exists in the atmosphere of the reactor building because the target debris from the reacted fuel pellet exits from the reactor cavity, along with the Xe in the cavity, through the beam port tubes into the containment building. After each microexplosion, purified Xe is introduced into the reactor cavity to reestablish 1 torr (133 Pa) of Xe pressure in the

cavity. Vacuum pumps at the perimeter of the containment building remove a similar amount of contaminated Xe from the building so that 1 torr of Xe pressure exists in the building. If good mixing is obtained, a steady-state tritium concentration of 1.7×10^{-6} g/m^3 (17 mCi/m^3) develops in the reactor building. This tritium inventory in the atmosphere of the building, containing 4.2×10^4 m^3, is only 72 mg (720 Ci).

The interior walls of the reactor containment building will be clad with thin sheets of stainless steel or aluminum in order to prevent the diffusion of tritium into the concrete. Because of the airborne tritiated gas in the atmosphere some of gases will adhere to these walls and all other exposed surfaces. A recent study[2] has measured the surface adsorption of tritium on stainless steel as a function of airborne concentration (in mCi/m^3) and indicates that the adsorption of HTO is much higher than for HT. The target debris in SIRIUS-M will principally exist as molecular DT. Based upon experimentally derived relationships for surface adsorption, the total DT adsorbed on the walls of the containment building (6×10^3 m^2) would be 3×10^{-6} g. The DT present will react, however, with water or oxygen present to form HTO. A known source of tritiated water will be contained in the purified Xe returning to the reactor cavity. The process for Xe purification removes tritium via oxidation followed by adsorption of the water. If the dryer beds are operated to assure a water pressure at the exit of the beds equivalent to a dew point of -60°C (1 Pa of H_2O), then the concentration of tritiated water in the building would be 16 mCi/m^3. The highest airborne concentration of HTO used in the cited study[2] was 1 mCi/m^3. If the adsorption increases linearly up to 16 mCi/m^3, then the total DTO adsorbed on the walls in the present case

Table 3.3-2. Tritium Inventory in Reactor Building

Location	Tritium, g
Captive Systems	
Fuel Injector	0.6
Breeder-Shield	8.0
Building Components	
Atmosphere	
as DT	0.07
as DTO	0.07
Surfaces	
as DT	1.5×10^{-5}
as DTO	5×10^{-4}
Graphite Cavity Liner	1.0
TOTAL	~ 10

would be 1 x 10^{-4} g. The values for surface adsorption are recorded in Table 3.3-2 multiplied by a factor of 5 to account for additional, unidentified surfaces which may be present.

Another exposed surface which will adsorb and retain tritium is the graphite tiles which cover the interior surface of the reactor cavity. These graphite tiles are directly exposed to the pellet debris; however, with the Xe gas in the cavity the high velocity tritium and deuterium ions are stopped before they reach the tiles. These ions do intersect the wall at a later time, however, as they are carried along by the blast wave, comparable to a kinetic energy beam of ~ 0.1 eV. Measurements of the retention of hydrogen in pyrolytic graphite exposed to low energy, ~ 0.35 eV, atomic beams of hydrogen[3] indicate that a significant inventory of hydrogen is obtained which reaches saturation very slowly. In addition, this low energy beam implantation reaches a maximum between 600 and 700 K which is approximately the average surface temperature for the graphite tiles, cooled to 500 K on the back side. Review of the data indicates that the hydrogen inventory in the graphite nearly reaches saturation of 20 x $10^{16}/cm^2$ at a fluence of 5 x $10^{19}/cm^2$, which will occur in the SIRIUS-M cavity in 10 full power days of operation. In this temperature range the hydrogen (tritium) retention by the low energy beam is approximately 4 times greater than for a deuterium beam at 100 eV, which reaches saturation more quickly.[4] This difference between the low energy and high energy atomic beams is attributed[4] to differences in the implantation mechanisms and subsequent diffusion and trapping of the hydrogen atoms in the graphite. Based upon the information from the low energy beam studies and the assumption that at saturation half of the hydrogen isotopes in

the graphite would be tritium atoms, approximately one gram of tritium would be retained in the graphite tiles at the end of reactor life.

3.3.3 Assessment of Tritium Radiological Hazard

The total inventory of tritium in the reactor building, ~ 10 g as given in Table 3.3-2, is an important consideration in assessing the potential environmental hazard of the facility as a result of an accidental release of tritium from the containment building. The hazards due to tritium release appear to be minimal because the amount of tritium is small and multiple, simultaneous failures of many systems would be required to cause much of the tritium to become airborne. In addition the building is operated below atmospheric pressure so that any leaks in the containment shell would cause external air to flood the containment building. The same logic can be applied to a rupture in a laser window separating the reactor building from the laser building which is operating at atmospheric pressure.

Perhaps the most severe accident would be for the aqueous breeder/coolant circuit to rupture so that all the water would flash-evaporate at 500 K. In such a scenario the building pressure would only increase to 0.9 atm so that the building would not be pressurized relative to the environment. If by some unknown mechanism, all the tritium were released (10 g), and vented through the stack at least 10 m high, then the maximum dose to an individual at the site boundary, 1 km, would be only 0.4 rem[5] which is below the 1 rem threshold required by the NRC to initiate an emergency evacuation plan. At a fully operational facility, however, the potential hazards of the reactor building would have to be considered along with all other potential hazards at the site.

References for Section 3.3

1. C.F. Henning et al., "TIBER-II/ETR Final Report," Lawrence Livermore National Laboratory, UCID-21150 (1987).

2. C.J. Sienkiewicz, "Tritium Surface Contamination," Fusion Technology, 8, 2444 (1985).

3. P. Hucks, K. Flaskamp and E. Vietzke, "The Trapping of Thermal Atomic Hydrogen on Pyrolytic Graphite," J. Nuclear Materials, 93&94, 558 (1980).

4. R.A. Causey, M.I. Baskes and K.L. Wilson, "The Retention of Deuterium and Tritium in POCO AXF-5Q Graphite," J. Vac. Sci. Tech., A4, 1189 (1986).

5. J.D. Lee, ed., "MiniMARS Conceptual Design: Final Report," Lawrence Livermore National Laboratory, UCID-20773, September 1986, Section 22.

4. IMPACT OF ENHANCED TARGET PERFORMANCE ON CAVITY DESIGN

4.1 Cavity Size for Enhanced Target

4.1.1. Response of Target Chamber Gas to Target Explosion

4.1.1.1. Introduction

In this section we consider the response of the target chamber gas to the exploding target. In the past, we have considered the response to the explosion of a 13.4 MJ target.[1] Here we present results for a target with a 100 MJ yield. As discussed above, we wished to study a higher yield target because it has a higher gain, so we could provide more neutrons for materials testing per joule of laser light from the driver. In this section, we present the target parameters, the absorption of target energy in the target chamber, the resulting pressure and thermal loading on the first wall.

4.1.1.2. SIRIUS-M Target

We consider the response target chamber gas to the explosion of a fusion target with a 100 MJ yield. The details of the target design influence the spectra of x-rays and ions that are emitted by the target, and therefore, affect the behavior of the target chamber gas. In this section, we will discuss the SIRIUS-M target and its debris ion and x-ray spectra.

We are considering the option of a 100 MJ target yield, so the target design is somewhat different than the 13.4 MJ base case design. The target is made of a hollow shell of frozen fuel surrounded by a plastic shell. The masses of the shells have been scaled from a 134 MJ target design.[2] The plastic shell contains 1.22 mg of CH_2, while there is 1 mg of DT fuel. We have assumed that this target will be driven to burn by a 1 MJ symmetrically applied pulse of short wavelength laser light, though we have done no calculations to substantiate this.

The 100 MJ yield is partitioned between x-rays, debris ions and neutrons. Table 4.1.1-1 shows that 75% of the energy is in neutrons, 19% is in ions, and 6% is in x-rays. This is typical for this type of target. The spectrum of x-rays is shown in Fig. 4.1.1-1 and the details of the debris ions appear in Table 4.1.1-2.

4.1.1.3. Absorption of Target Energy in Target Chamber Gas

The energy released by the burning target spreads throughout the target chamber and the entire SIRIUS-M facility. The neutrons, which are responsible for 75% of the target yield, deposit energy mainly in the first wall, test modules, reflectors, and shields. The target chamber first wall and cavity gas, which is 1 torr of xenon gas, absorb the target generated x-rays. The cavity gas stops virtually all of the debris ions.

We have used the CONRAD[3] computer code to simulate the deposition of target generated x-rays and ions in the target chamber gas. CONRAD is a Lagrangian hydrodynamics computer code with multigroup radiation transport and x-ray and ion deposition physics. Table 4.1.1-3 shows the x-ray and ion energies absorbed in the target chamber gas for first wall radii of 3, 4, and 5 meters. For all three radii, virtually all of the x-ray and ion energy is absorbed in the gas. The deposition of this energy leads to the gas temperature profile shown in Fig. 4.1.1-2. One sees in this figure that the bulk of the energy is stopped within 100 cm of target chamber gas. The gas, once it contains this temperature profile, radiates thermal energy and transmits a shock to the first wall.

4.1.1.4. Mechanical Load on Target Chamber Walls

We have used the CONRAD computer code to simulate the generation, propagation, and reflection from the wall of the shock wave associated with

Table 4.1.1-1

SIRIUS-M Target Energy Partition

Fusion Energy = 100 MJ

Neutron Energy = 75 MJ

Debris Energy = 19 MJ

Radiated Energy = 6 MJ

Table 4.1.1-2

Target Debris Ions

Ion Species	# of Ions ($\times 10^{20}$)	Ion Energies (keV)	Total Energy (MJ)
D	1.0	93	1.4
T	1.0	140	2.0
He	.75	180	2.0
C	.52	1600	11.6
H	1.0	140	2.0

Table 4.1.1-3

SIRIUS-M Target Chamber Gas Behavior

	Radius of First Wall		
	3 meters	4 meters	5 meters
X-ray Energy Absorbed in Gas (MJ)	5.8	5.9	5.9
Ion Energy Absorbed in Gas (MJ)	19.9	20.2	20.4
Energy Reradiated to First Wall (MJ)	24.3	22.4	19.2
Maximum Pressure on First Wall (MPa)	.0015	.0022	.0013

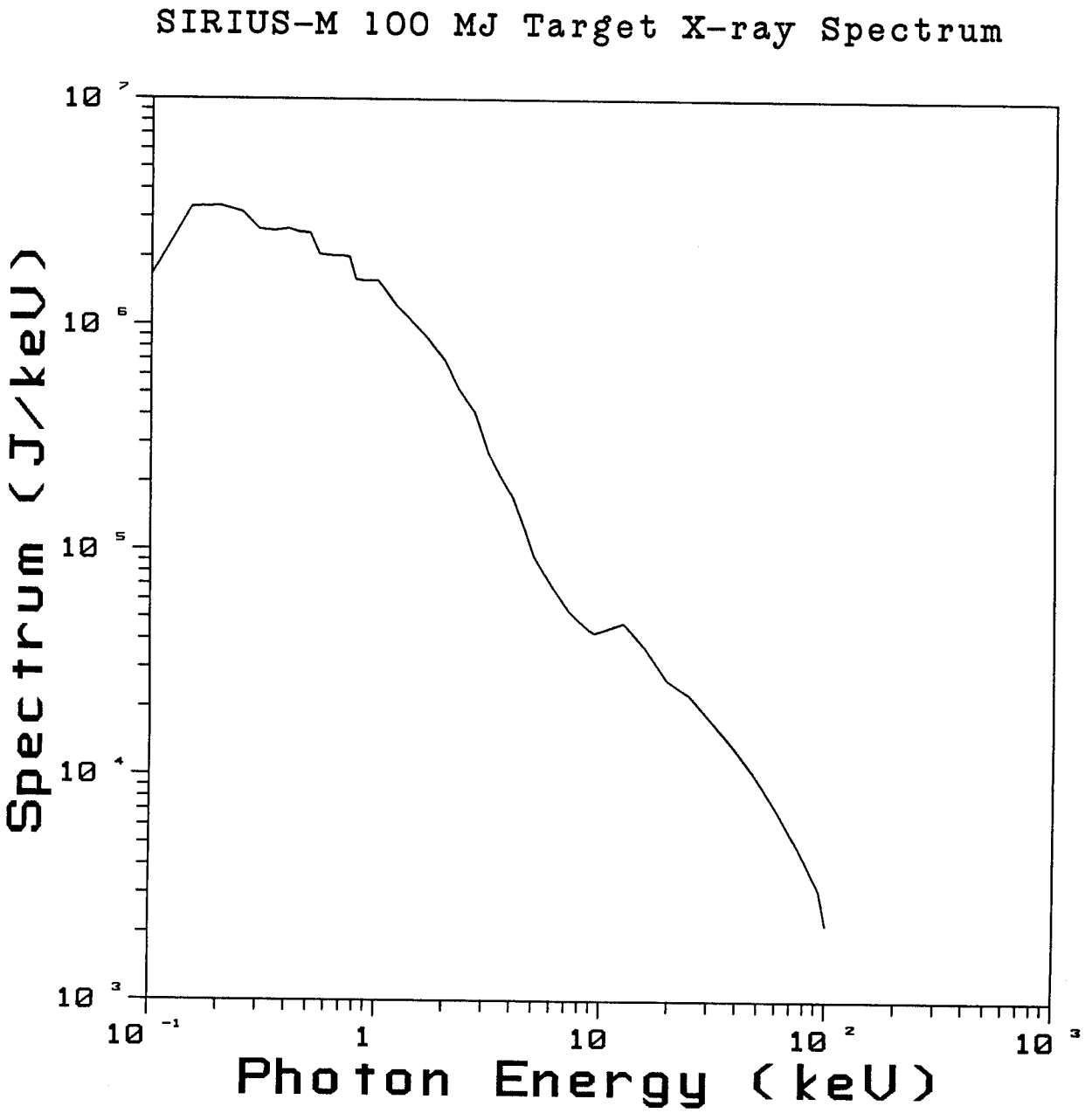

Figure 4.1.1-1. Spectrum of X-Rays from SIRIUS-M Target.

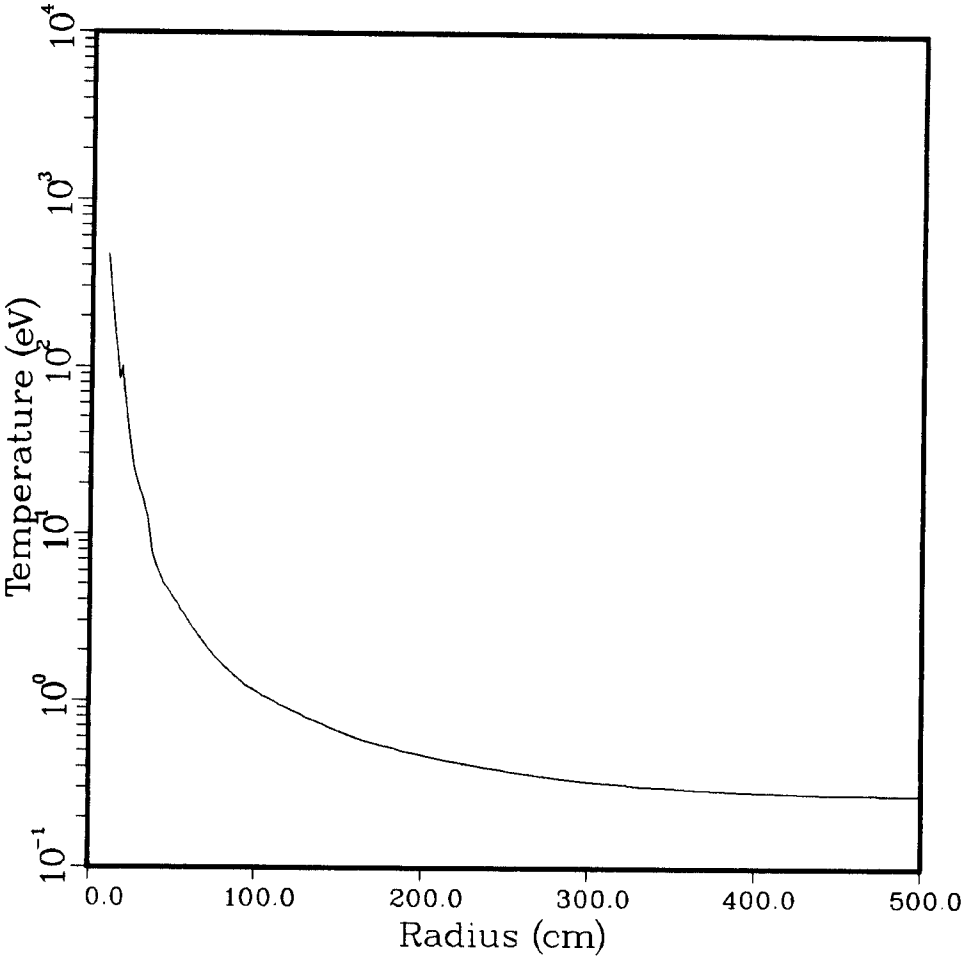

Figure 4.1.1-2. Plasma Temperature Profile in 1 Torr Xenon Gas at Conclusion of SIRIUS-M Target X-Ray and Debris Ion Deposition.

the initial temperature profile of Fig. 4.1.1-2. We have done these calculations for first wall radii of 3, 4, and 5 meters. We show the pressure on the first wall as a function of time for the three cases in Fig. 4.1.1-3. The maximum pressures on the walls are listed in Table 4.1.1-3. These pressures are so low that they are inconsequential to the survival of the first wall.

It is interesting to note that the pressure pulse for the 3 meter radius target chamber does not have the characteristic shape of a well formed shock. Evidently, the shock driven by the temperature profile in Fig. 4.1.1-2 needs to propagate between 3 and 4 meters before it becomes a typical shock.

4.1.1.5. Heat Load on Target Chamber Walls

We have also used CONRAD to simulate the emission of radiation from the target chamber gas and the propagation of this radiation to the first wall. The radiation heat fluxes on the first wall are shown in Fig. 4.1.1-4 for wall radii of 3, 4, and 5 meters. The time-integrated energy radiated to the first wall is given in Table 4.1.1-3. Virtually all of the energy absorbed by the gas is reradiated. The peak radiant flux is lower for the larger radii because roughly the same power radiates to a larger surface. The large amounts of radiant energy can thermally damage the first wall, which is the subject of the remainder of section 4.1.

4.1.2 First Wall Thermal Response

The thermal responses of the graphite first wall in SIRIUS-M with 100 MJ target were calculated for different cavity radii to determine the cavity radius such that the first wall would be operating under acceptable thermal and stresses conditions. As described above, the released energy spectra of

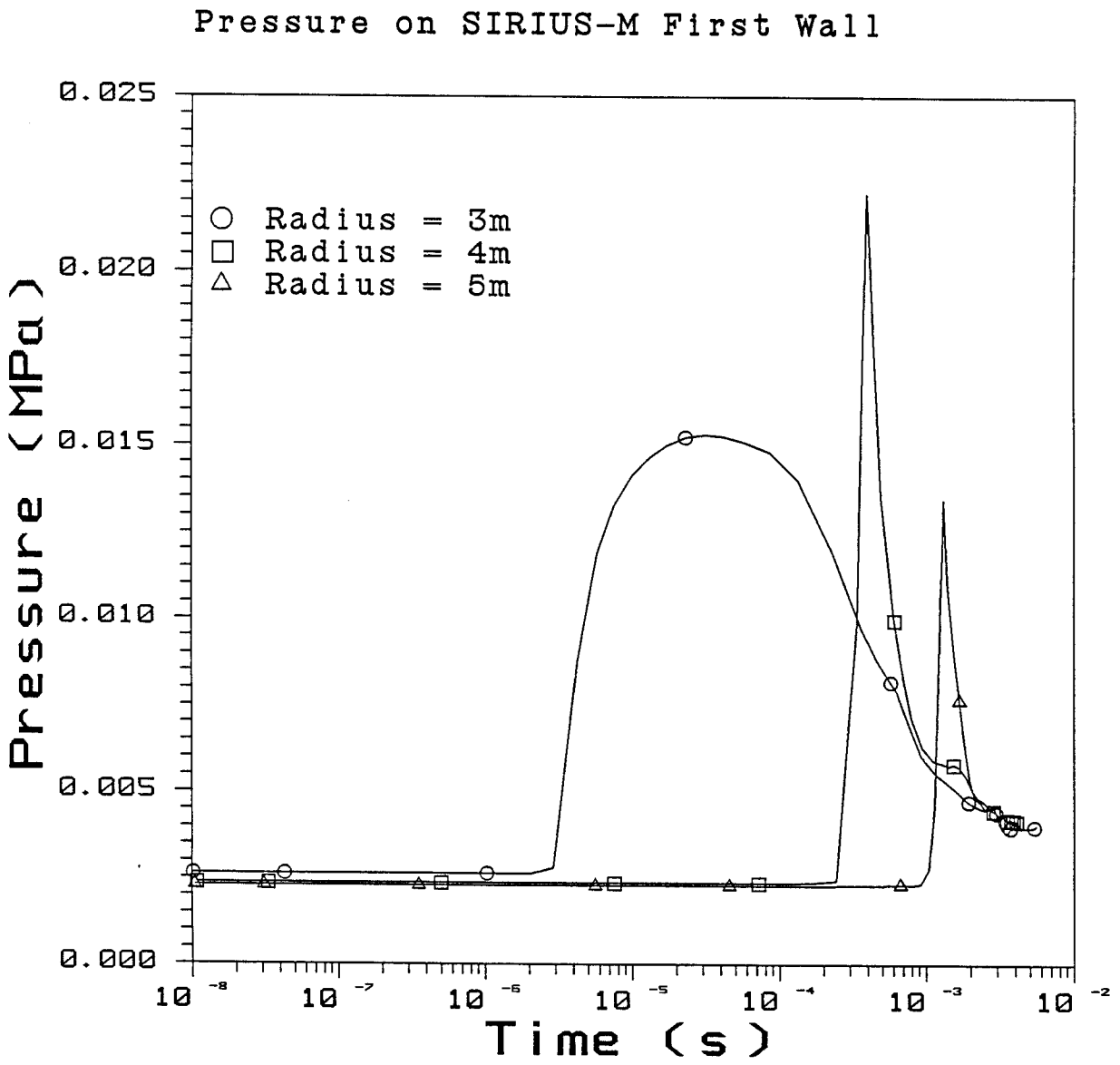

Figure 4.1.1-3. Pressure on SIRIUS-M Target Chamber Walls versus Time. Wall radii are 3, 4, and 5 meters.

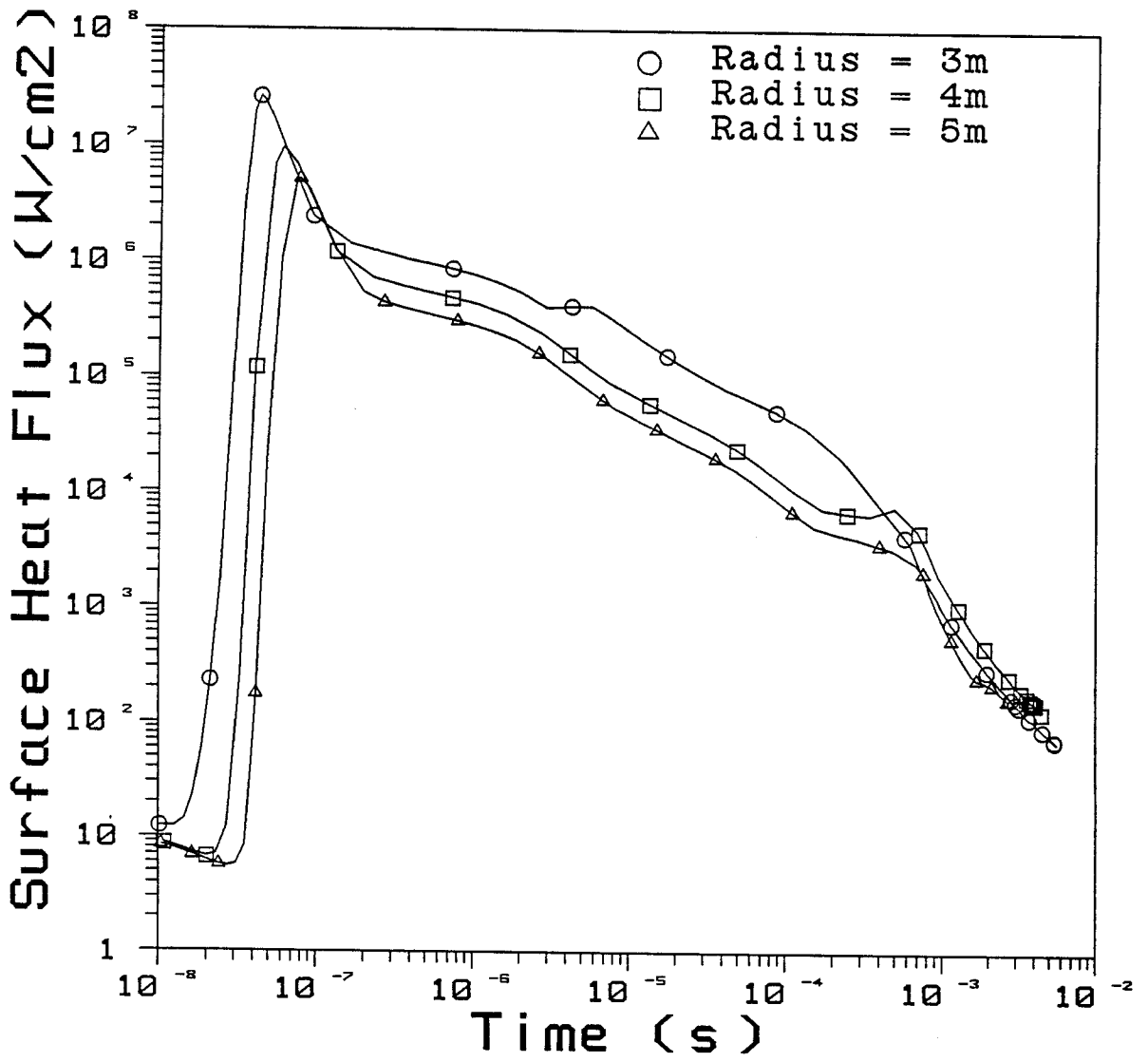

Figure 4.1.1-4. Surface Heat Flux on SIRIUS-M Target Chamber Walls versus Time. Wall radii are 3, 4, and 5 meters.

the 100 MJ target were scaled directly from the 13.4 MJ target spectra used in the previous SIRIUS-M[1] study. However, the reflected laser light from the target to the first wall is assumed[2] here to be 7% of the incident laser energy (1 MJ) on the target, versus 10% used in SIRIUS-M.

The energy deposited on/in the first wall consists of the reflected laser light and the energy leaked and reradiated from the 1 torr xenon gas used in the target chamber. The leaked energy is mainly due to the soft x-ray, and in the case of the smallest radius considered (3 m), a small fraction of the carbon ions reaches the first wall after being slowed down in the xenon gas. The reradiated energy of the gas was obtained from the calculations described in the previous section. The computer code ATEN,[4] used in these calculations, calculates the energy deposition in the gas and in the first wall and with the supplied heat flux from the CONRAD code, calculates the temperature response of the first wall.

The temperature rise (ΔT) at the front surface of the first wall is shown in Fig. 4.1.2-1 for 3, 4, and 5 m radius cavities for 500° K steady-state back surface temperature. The first three peaks in each case are due to the reflected laser light, and after which the temperature decreases until the arrival of the reradiated heat flux that marks the highest temperature rise in each case. The maximum temperature rises at the front surface are 2260, 993, and 610°F for the 3, 4, 5 m radius cavities respectively. The evaporation of the graphite was negligible in the three cases.

Unlike the 13.4 MJ case, where the maximum temperature was due to the reflected laser light, the maximum temperatures in these cases are due to the reradiated heat flux. This is expected, since the energy caused by the ions

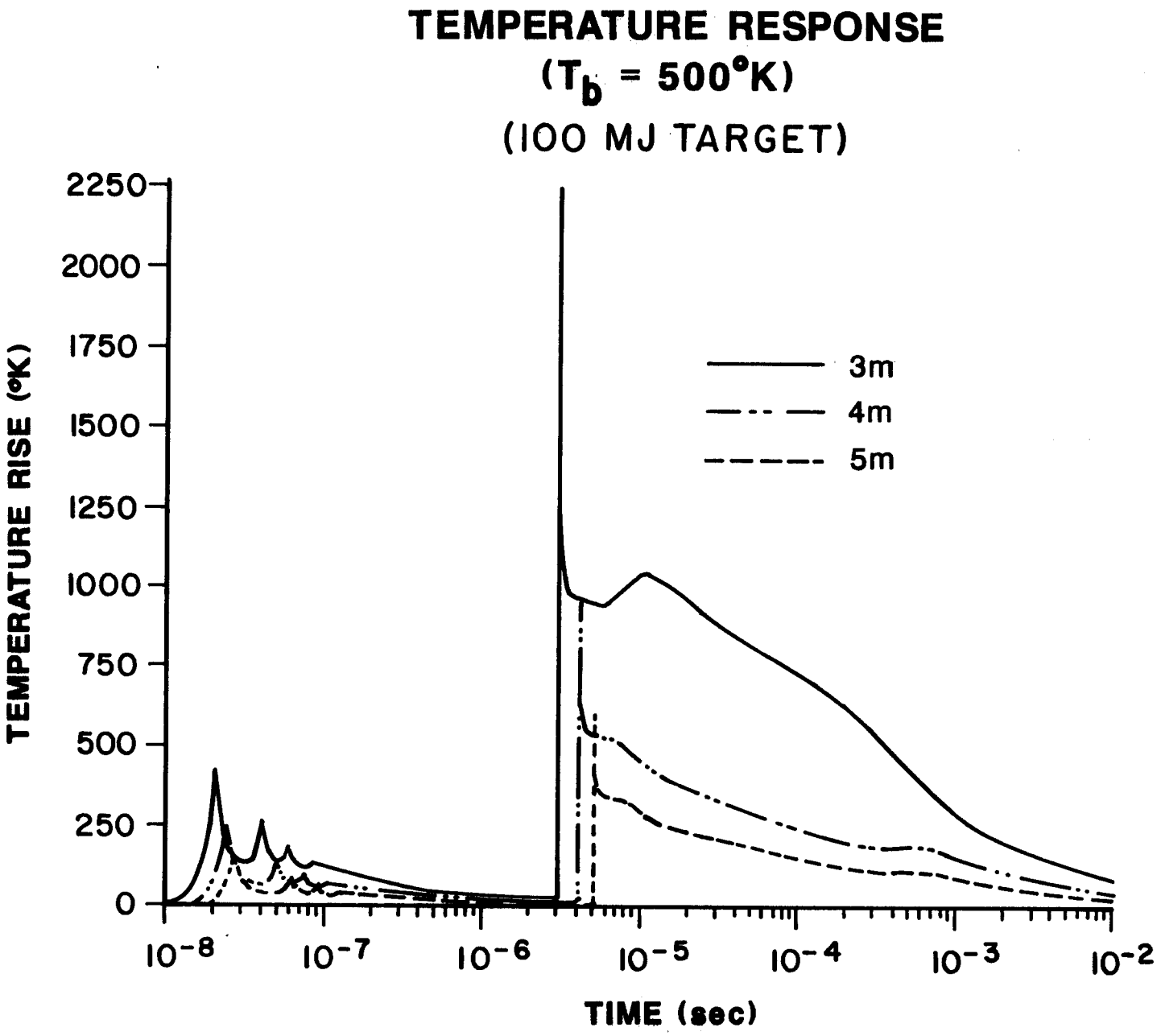

Figure 4.1.2-1. Temperature rise at the first wall front surface for the 100 MJ target and for 3, 4, and 5 m wall radii.

(and consequently the heat flux) in the 100 MJ target design is about 7.5 times the ions' energy in the 13.4 MJ target. Conversely the reflected laser light is decreased by about 30%. The resulting thermal stresses from these temperature profiles are considered in the next section.

4.1.3 Thermal Stresses

Energy deposition in the first wall tiles produces an extremely steep temperature gradient and a corresponding distribution of thermal stress. The state is biaxial, with equal principal values and a response which is elastic. Since only a thin layer is highly stressed, the thermal deflection of first wall components from the initial deposition is negligible. The program for calculating thermal stress includes the temperature-dependence of material properties. In the case of graphite, strength and stiffness both increase as it is heated. The design criterion uses the condition that the induced thermal stress must not exceed the compressive strength at a given temperature.

Results are shown in Fig. 4.1.3-1 for graphite with back surface temperatures of 500 K and 773 K. With decreasing radii, the tile strength rises due to the increasing maximum first surface temperature change. However, peak thermal stress increases at a faster rate, with the design limit reached at radii of 3.65 m and 3.80 m for back temperatures of 500 and 773 K. The figures also include the corresponding variation in safety factor (ratio of strength to stress) with practically the same rate of change with respect to radius.

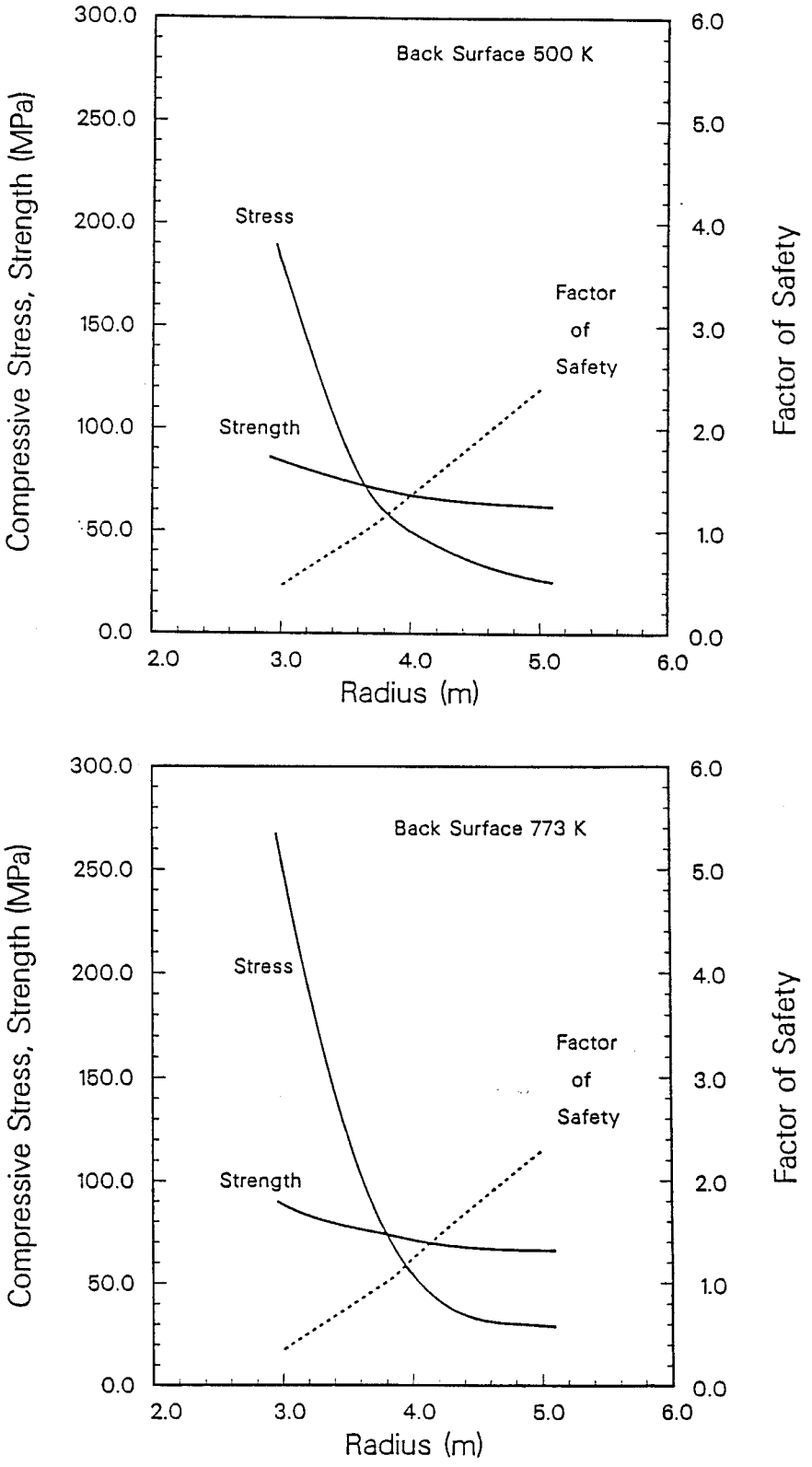

Figure 4.1.3-1. Compressive stress in graphite tiles as a function of cavity radius for back surface temperatures of 500 K and 773 K.

Similar calculations were also made for a beryllium first wall, with results shown in Fig. 4.1.3-2. It can be seen that the surface temperature rise coincides with the melting condition for a radius of 3.54 m. The thermal stress was found to be considerably greater than the compressive yield strength for the relevant range of parameters. The relatively poor performance of beryllium may be clarified by comparing a figure of merit (F) for thermal pulse loading of material surfaces

$$F = S(1 - \mu)\ (\rho c k)^{1/2}/\alpha E\ .$$

Here S, μ, ρ, c, k, α and E denote strength, Poisson's ratio, density, specific heat, conductivity, expansivity and elastic modulus, respectively. In Table 4.1.3-1 a comparison is made between typical candidate first wall materials. Units for F are $MW \cdot s^{1/2}/m^2$ with properties evaluated at 1000 K. An order of magnitude difference is apparent between beryllium and the best material, graphite.

References for Section 4.1.1, 4.1.2 and 4.1.3

1. B. Badger, et al., "SIRIUS-M: A Symmetric Illumination, Inertially Confined Direct Drive Materials Test Facility," University of Wisconsin Fusion Technology Institute Report UWFDM-651 (September 1985).

2. L. Lund, University of Rochester, private communication, October 1983.

3. R. Peterson, "CONRAD - A Combined Hydrodynamics-Condensation/Vaporization Computer Code," University of Wisconsin Fusion Technology Institute Report UWFDM-670 (April 1986).

4. H. Attaya, to be published.

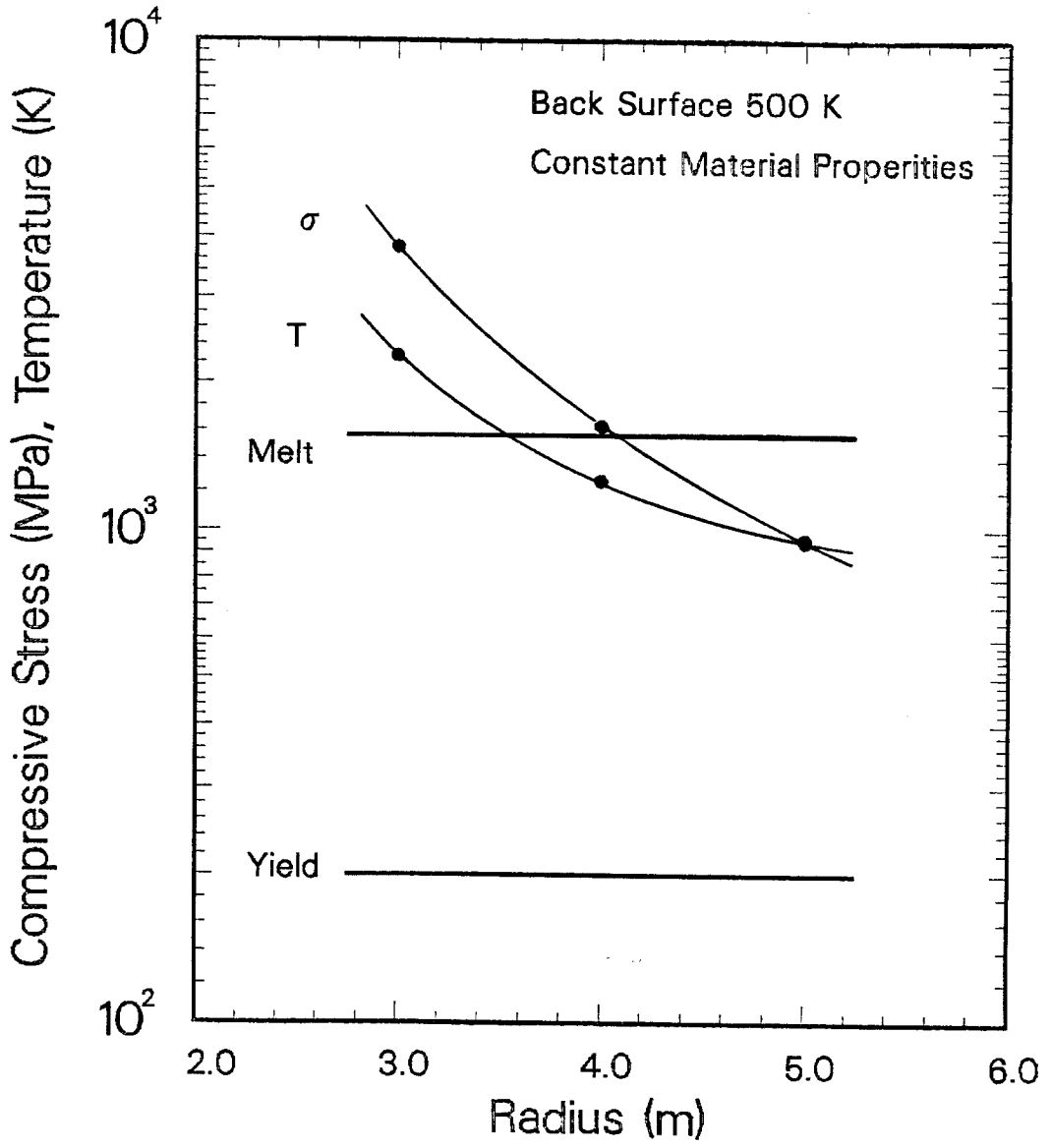

Figure 4.1.3-2. Compressive stress and temperature vs. radius for beryllium first wall.

Table 4.1.3-1. Thermal Stress Resistance of Pulsed First Wall Materials

Material	F
Graphite	22.0
Silicon Carbide	8.0
Titanium Carbide	7.8
Boron Carbide	7.8
Zirconium Carbide	4.3
Beryllium	1.9
Beryllium Oxide	1.6

4.2 Economic Impact of Enhanced Target Performance

In order to understand the cost differences between the base case of a 13.4 MJ, 2 m test reactor and this new case of a 100 MJ test reactor (without tritium breeding), Table 4.2-1 has been prepared. It compares the cost of the items affected for the two facility designs. There are other cost components that are not affected by the switch to a higher yield target and a larger radius cavity. In this example, the rep rate is kept constant at 10 Hz, so the cavity radius is increased to 5.5 m in order to conserve the wall loading.

Because the constant rep rate is associated with a higher target yield, the fusion power of the new case goes up in proportion to the target yield.

The dependences of cost on the fusion power and the cavity radius can be separated, because cost of certain items depends only on fusion power, while the cost of some other items (cavity materials) depend exclusively on the cavity radius; the rest of the cost items are independent of these two parameters. Table 4.2-1 presents the breakdown in cost for the items that are affected by this change in the facility design and compares the bare direct cost of the whole facility between the 13.4 MJ and the 100 MJ cases.

Parametric Studies of Direct Cost of a 100 MJ Facility Without Breeding

Figure 4.2-1 presents the results of parametric studies of direct cost for a 100 MJ facility without tritium breeding. It presents the direct cost as a function of rep rate, with the cavity size as a parameter. Since the direct cost of the facility C can be written as:

$$C = C_0 + C_1(R^2) + C_2(\nu)$$

Table 4.2-1. Comparison of a 100 MJ and a 13.4 MJ Design Without Breeding

E_0 = 13.4 MJ E_1 = 100 MJ

r_0 = 2 m r_1 = 5.5 m

ν_0 = 10 Hz ν_1 = 10 Hz

		Direct Costs ($M)		
	Affected Item	Before	Now	Scaling Law(1)
1)	Cooling system structures	4.6	7.3	\$9.05 M x $(Pg/1000)^{0.3}$
2)	Heat rejection	6.0	20.4	\$145 K x $Pg^{0.8}$
3)	Part of electrical plant	3.9	29.1	C_{ref} x $P_{aux}/P_{ref,aux}$
4)	Miscellaneous plant	23.2	33.6	\$5.05 M x $Pg^{0.3}$
5)	I&C	13.6	22.0	\$2.52 M x $P_{th}^{0.3}$
6)	Maintenance equipment	22.1	35.8	\$4.1 M x $P_{th}^{0.3}$
7)	Graphite	4.1	30.6	\$4520/kg
8)	Pb	1.9	14.2	\$4.5/kg
9)	PCA	11.8	88.1	\$50/kg
10)	Pb pumps	2.7	20.1	\$27.45 M x $\dot{m}/3.2 \times 10^8$ kg/hr
11)	Pb heat exchangers	4.2	31.3	\$81.2 M x $P_{th,Pb}$/2081 MW
12)	Pb cleanup	3.3	24.6	\$7.5/kg
13)	H_2O pumps	3.6	26.9	\$264 K/1.0 x 10^5 kg/hr
14)	H_2O heat exchangers	3.3	24.6	\$31.8 M x $P_{th,w}$/730 MW
15)	Auxiliary cooling	0.9	6.7	C_{ref} x $P_{aux}/P_{aux,ref}$
		\$109.2 M	\$415.3 M	

Δ = \$306.1 M

BDC_0 = \$452 M

BDC_1 = \$758 M (+67.7%)

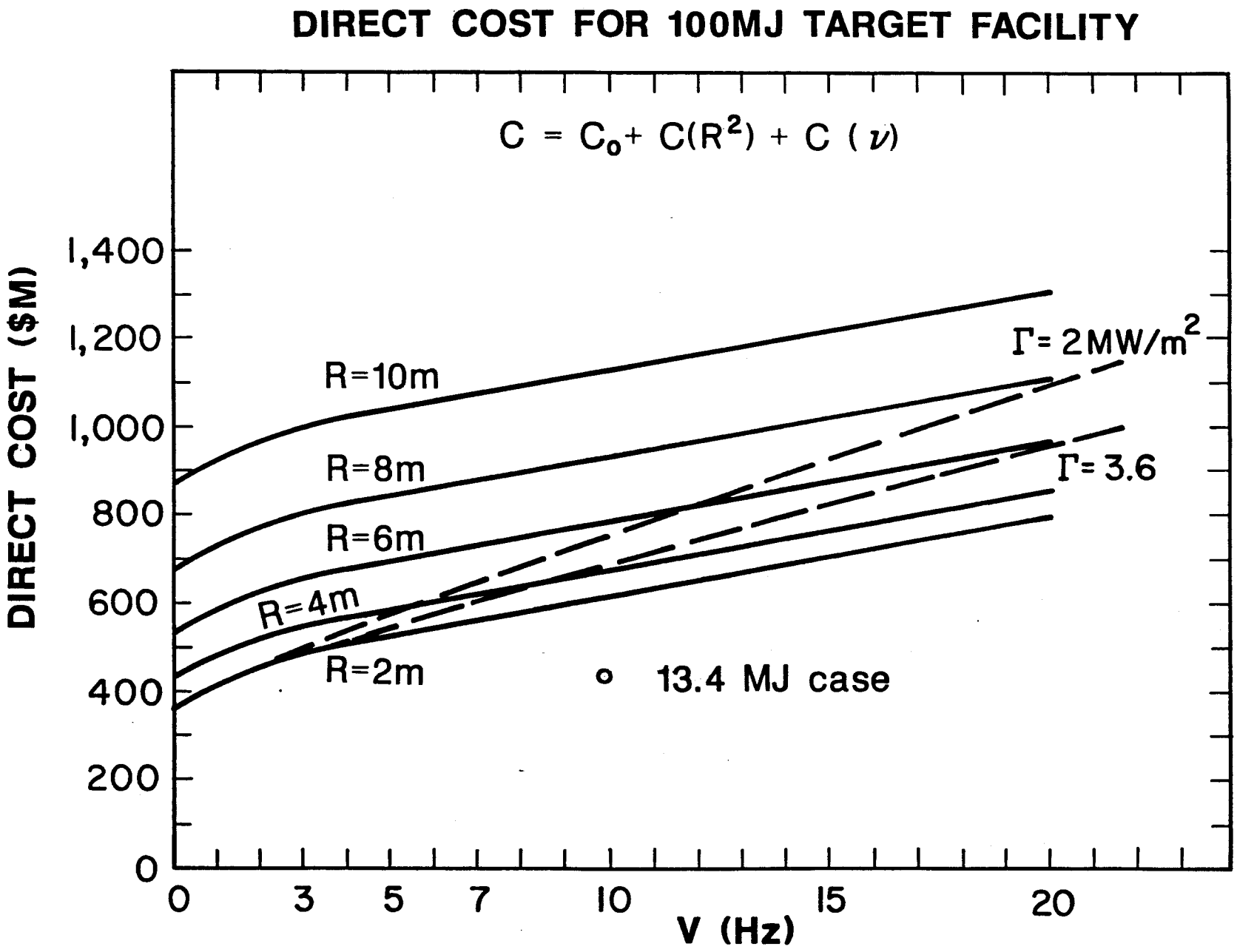

Fig. 4.2-1. Parametric study of cost with respect to cavity radius and rep rate for the 100 MJ facility.

where: R = cavity radius

ν = rep rate

then the dependences on R and ν can be separated from each other. The dependence on the rep rate is approximately linear for $\nu > 3$ Hz and the dependence on the cavity size is approximately quadratic, as can be seen from the figure. Also shown in Fig. 4.2-1 are the boundaries (in dashed lines) imposed by the condition that the wall loading, Γ, should be between 2 MW/m^2 and 3.6 MW/m^2. From other considerations, the minimum cavity size for a 100 MJ target yield should be about 4 m. In order to satisfy the wall loading considerations, we are interested in the section of the 4 m curve on Fig. 4.2-1 that is between the 2 MW/m^2 and 3.6 MW/m^2 dashed lines. Therefore the rep rate should be between 5.36 Hz and 9.65 Hz and the corresponding bare direct cost (BDC) of the 100 MJ facility lies in the range of \$590 M - \$670 M (for the 13.4 MJ facility the BDC was \$452 M). Therefore the increase in cost over the base case is substantial (30.5% to 48.2%). The data used in generating Fig. 4.2-1 are shown in Table 4.2-2.

Figure 4.2-2 presents the figure of merit (FOM - defined below) and the cumulative damage (in dpa-ℓ) for the 2 m and the 4 m 100 MJ reactor without breeding as a function of rep rate. Also shown on the same graph are the data for our base case (2 m, 13.4 MJ target). The solid lines show the cumulative damage function for these two cases (the corresponding ordinate is on the left) and the points marked "X" show the cumulative damage (in dpa-ℓ) for the 2 m base case and for the 1.5 m 13.4 MJ case. The dashed curves show the figure of merit (FOM) for the 2 m and 4 m 100 MJ reactor costs. The FOM is a decreasing function of rep rate because the cumulative damage increases with

Table 4.2-2. Parametric Studies for a 100 MJ Yield

Direct Costs Shown in $M

	Hz		ν = 0	3	5	7	10	15	20
	m	Dependence	R = 0	2	4	6	8	10	
1) Cooling system structures		ν	0	5.4	6.1	6.7	7.3	8.2	8.9
2) Heat rejection		ν	0	9.3	12.8	16.1	20.8	28.1	34.9
3) Part of elec. plant		ν	0	8.7	14.6	20.4	29.1	43.7	58.2
4) Miscellaneous plant		ν	0	26.0	28.7	30.8	33.6	37.2	40.2
5) I&C		ν	0	16.3	18.5	20.3	22.4	25.2	27.3
6) Maintenance eq't.		ν	0	26.5	30.1	33.0	36.4	41.0	44.4
7) Heat transfer equipment		ν	0	32.9	54.9	76.8	109.7	164.6	219.4
Subtotal		ν	0	125.1	165.7	204.1	259.3	348.0	433.3
Reactor Cavity Total		R	0	21.1	84.4	189.9	337.6	527.5	

Rest: $342.8 M

Fig. 4.2-2. Parametric study of cumulative damage and figure of merit (FOM) with respect to cavity radius and rep. rate for the 100 MJ facility.

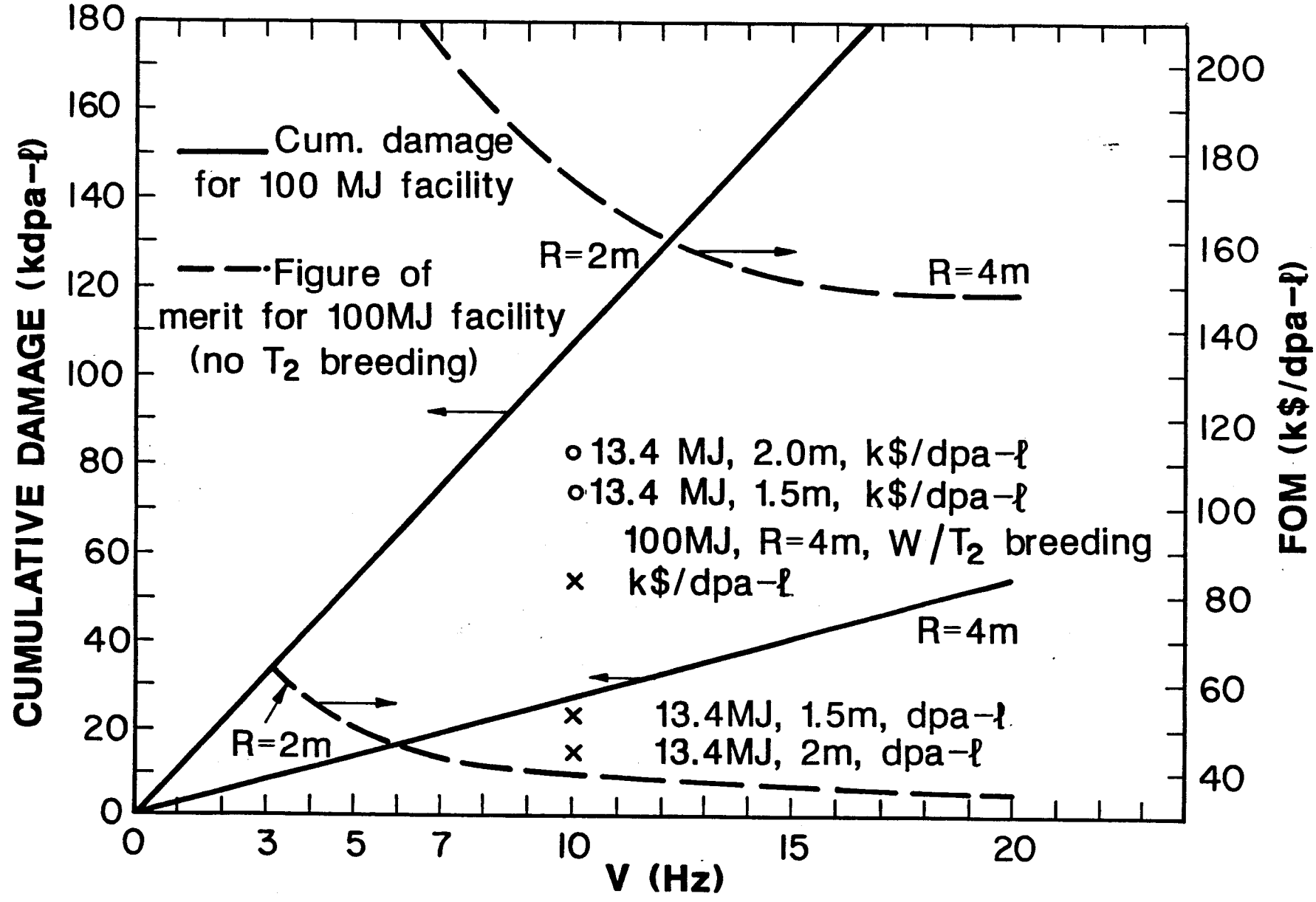

fusion power. The FOM is defined as the ratio of the total lifetime cost (total overnight cost plus the sum of all the annual costs over the life of the plant) and the cumulative damage. Points marked "O" on the figure are the FOMs for the two 13.4 MJ cases. As can be seen, at 10 Hz the 100 MJ, 4 m reactor has a much worse FOM than our base case. However, this FOM is improved substantially (and is actually better than the FOM for the base case design) if tritium breeding is included in the design (point marked "*"). The reason for this is that due to increase in the fusion power, the fuel requirements, and consequently the fuel cost, of the 100 MJ 10 Hz facility is enormous (a cost of $271 M per year for fuel alone). This drives up the total annual cost and hence the FOM. On the other hand, with tritium breeding equipment, this cost drops to zero in exchange for ~ $10 M in additional bare direct cost. Therefore, this option cuts the FOM of the 100 MJ, 4 m, 10 Hz reactor by 52%.

The 100 MJ and the 13.4 MJ designs with various breeding scenarios are shown in Tables 4.2-3 and 4.2-4 . Table 4.2-4 assumes zero fuel credit for T_2 bred. The 100 MJ cases shown are the rep rate of 5.36 Hz (which keeps the wall loading at 2 MW/m^2) and 1.34 Hz (which keeps the fusion power at 134 MW, the same as the 2 m base case, though the wall loading may be below the required value). Shown are the bare direct cost (BDC), total overnight cost (TOC) and components of the annual cost (operations and maintenance, fuel and electricity). Fuel credit in Table 4.2-3 is given at the same rate that the fuel cost is charged -- at 10,000/g of T_2. The total lifetime cost is defined as the sum of TOC and the annual costs summed over the life of the facility (10 yr). The FOM is then the ratio of the total lifetime cost and the total

Table 4.2-3. Comparisons in Costs and FOM Among Various Breeding Alternatives for the 13.4 MJ, 2 m and 100 MJ, 4 m Designs; Fuel Credit Given at $10,000/g of T_2

FOM_1 = 0.277 BDC + AC

Type Cost ($M)	Original 2 m	1	2	3	4	5	6	1	4	6	1	4	6
		2 m With Breeding						100 MJ, 4 m, 1.34 Hz With Breeding			100 MJ, 4 m, 5.36 Hz With Breeding		
BDC	452	452	446	455	443	460	464	528	493	542	573	538	620
TOC	855	855	844	861	838	870	878	999	933	1025	1084	1018	1173
O&M	25.5	25.5	25.2	25.7	25.0	26.0	26.2	30.0	28.0	30.8	32.5	30.5	35.2
Fuel	36.3	-14.4	-2.75	-2.8	-4.8	-5.6	-10.7	-14.4	-4.8	-10.7	-57.6	-19.2	-42.8
Electricity	13.2	13.2	13.2	13.2	13.2	13.2	13.2	1.8	1.8	1.8	7.1	7.1	7.1
Total Annual Cost, AC	75.	24.3	35.6	36.1	33.4	33.6	28.7	17.4	25.0	21.9	-18.0	18.4	-0.5
Total Lifetime Cost	1605	1098	1200	1222	1172	1206	1165	1173	1183	1244	904	1202	1168
Cum. Damage dpa-ℓ	14200	11232	11175	13689	11289	11985	11985	2808	2822	2996	11232	11289	11985
FOM (k$/dpa-ℓ)	113	97.8	107.4	89.3	103.8	100.6	97.2	418.	419.	415.	80.5	106.5	97.5
FOM_1 ($M)	200	149.5	159.1	162.1	156.1	161.0	157.2	163.7	161.6	172.0	140.7	167.4	171.2

Table 4.2-4. Comparisons in Costs and FOM Among Various Breeding Alternatives for the 13.4 MJ, 2 m and 100 MJ, 4 m Designs; No Fuel Credit Given

$FOM_1 = 0.277\ BDC + AC$

Type Cost ($M)	Original 2 m	2 m With Breeding						4 m, 100 MJ, 5.36 Hz With Breeding					
		1	2	3	4	5	6	1	2	3	4	5	6
BDC	452	452	446	455	443	460	464	573	550	586	538	604	620
TOC	855	855	844	861	838	870	878	1084	1040	1108	1018	1143	1173
O&M	25.5	25.5	25.2	25.7	25.0	26.0	26.2	33.7	31.2	33.0	31.7	34.3	36.5
Fuel	36.3	0	0	0	0	0	0	0	0	0	0	0	0
Electricity	13.2	13.2	13.2	13.2	13.2	13.2	13.2	7.1	7.1	7.1	7.1	7.1	7.1
Total Annual Cost, AC	75.	38.7	38.4	38.9	38.2	39.2	39.4	40.8	38.3	40.3	38.8	41.4	43.6
Total Lifetime Cost	1605	1242	1228	1250	1220	1262	1277	1492	1423	1511	1406	1557	1609
Cum. Damage dpa-ℓ	14200	11232	11175	13689	11289	11985	11985	11232	11175	13689	11289	11935	11985
FOM (k$/dpa-ℓ)	113	111	110	91	108	105	106	133	127	110	125	130	134
FOM_1 ($M)	208	164	162	165	161	167	168	200	191	203	188	209	215

cumulative damage in dpa-ℓ. An alternative figure of merit, which more truly reflects the cost of borrowed money under the assumptions used, is also shown. This FOM doesn't incorporate the cumulative damage, because a certain minimum wall loading (~ 2 MW/m^2) is required and damage rate (in dpa/y) is proportional to the wall loading. This FOM is the annual cost (including borrowed money) of owning and operating the facility.

Based on the old figure of merit, the best configuration is for the 100 MJ, 4 m, 5.36 Hz design with a 30 cm multiplier zone with Be balls and H_2O cooling with 20 g/100 cc dissolved $LiNO_3$ as the breeder; this is followed closely by the 2 m, 13.4 MJ, 10 Hz design with the liquid Pb zone with H_2O shield and first wall cooling containing 80 g/100 cc $LiNO_3$. If the alternative FOM is used, then the best case is the same as above (100 MJ, 4 m, 5.36 Hz, 30 cm Be zone and 20 g/100 cc $LiNO_3$) followed very closely by the 13.4 MJ, 2 m, 10 Hz case with the same cavity configuration. If no fuel credit is allowed for bred T_2, and if a minimum wall loading of ~ 2 MW/m^2 is required, then by far the best case is the 13.4 MJ, 2 m, 10 Hz design with a 30 cm solid lead multiplier zone cooled by H_2O with 20 g/100 cc dissolved $LiNO_3$ as the breeder. If there is no market for bred T_2, then the object is to reduce the amount of T_2 produced and the best case is the 13.4 MJ, 2 m, 10 Hz design with a 30 cm liquid lead zone and H_2O cooling elsewhere with 80 g/100 cc dissolved $LiNO_3$ for the breeder. However, in that case the price of T_2 purchased would probably be low, and if we don't want to introduce any additional T_2 into the economy, then the base case (2 m cavity without breeding) is the only case to be considered.

The cost of T_2 produced in the breeding options for SIRIUS-M can be legislated as has been done above (at \$10,000/g or \$0/g) or it can be calculated as will be shown here.

The cost of producing T_2 will have several components:

a. The cost of raw material, which in this case will be the cost of burned Li. Assuming we have 90% enriched Li as the worst case, we know that the cost of this is \$1200/kg. For each g of T_2 produced, approximately 2 g of Li are consumed. If we are producing 10 kg of T_2 (about the upper limit for the SIRIUS-M options considered), then we are consuming 20 kg of Li/year and the cost is only \$24,000/y. Therefore, raw material cost is a very minor item.

b. Cost of additional (breeding) equipment levelized (depreciated) over plant lifetime. If we charge just the cost of the breeding equipment to the selling price of T_2, and charge the other option-dependent costs in Table 2.2-2 to the operation of our basic facility, and with the economic assumptions used in this study,[1] this item comes out to \$2.0 M/y.

c. The cost of operating and maintaining this additional equipment, given these economic assumptions is about \$0.4 M/y.

Therefore the total cost of T_2 production would be \$2.4 M/y. The selling price of T_2 produced (assuming no profit margin for this government owned facility) would depend on the amount produced. This price is given in Table 4.2-5 for the various design options considered. It is shown that the selling price of a T_2 producing ETR can be substantially less than the currently prevailing price of \$10,000/g.

Table 4.2.5. Selling Price of T_2 in $/g

	2 m, 13.4 MJ Facility		4 m, 100 MJ Facility		
Case from Table 2.2-1	TBR	Price @ 10 Hz	Price @ 1.34 Hz	5.36 Hz	10 Hz
1	1.399	1767	1767	442	237
2	1.076	9251	9251	2313	1240
3	1.077	9118	9118	2280	1222
4	1.132	5322	5322	1331	713
5	1.154	4567	4567	1142	612
6	1.296	2373	2373	593	318

References for Section 4.2

1. Zoran Musicki, "The Economic Analysis of SIRIUS-M, A Symmetrically Illuminated Inertial Confinement Fusion Engineering Test Reactor," UWFDM-708, September 1986.

5. ECONOMIC SCALING OF SIRIUS-M TO "DEMO"

5.1 Design Parameters for a DEMO

The definition of a DEMO is a reactor which has a power output on the lower range of typical commercial units, which can demonstrate power generation and conversion at a reasonable efficiency and can do it at a reasonable availability.

Typically, conceptual fusion reactor studies have shown a strong economy of scale with respect to cost of electricity, favoring electrical outputs > 1000 MWe. A DEMO, however, does not need to produce economically competitive cost of electricity. It needs only to demonstrate that it extrapolates to an economically competitive system. This will be done during the design and development phase of DEMO and during early operation. Commercial reactors must have an availability of 65-75% to be economically competitive. A DEMO should have an availability of > 50% and should show straightforward extrapolation to 65-75%.

In addition to the above, a DEMO should demonstrate all the technologies to be used in commercial reactors. Thus it must have a capability of a breeding ratio > 1.0, T_2 extraction, containment and processing. It must also have remote handling capability for maintaining all the systems which can fail during operation and which cannot be serviced hands on.

It is interesting to give a historical perspective on former DEMO reactors. The French Phénix LMFBR had a power output of 230 MWe, the Clinch River LMFBR (which was never constructed) 350 MWe and the Fort St. Vrain HTGR DEMO, 330 MWe. We feel that a fusion power of 1000 MW_{th} producing 350-450 MWe appears appropriate for our design. The following parameters have been used in the costing:

Fusion power (MW_{th})	1000
Laser energy (MJ)	1.0
Target gain	100
Rep. rate (Hz)	10
Availability (%)	50-75
Construction time (y)	6
Plant lifetime (y)	20

5.2 Cost Estimate of "DEMO" Facility

A 100 MJ, 4 m, 10 Hz demo plant has been costed using a design similar to the base case 13.4 MJ, 2 m, 10 Hz with breeding. Table 5.2-1 presents the difference in cost of affected items. The change in assumptions is that now the availability is assumed to be 75%, construction time is 6 years and plant lifetime is 20 years. This demo produces ~ 366 MWe of net power.

Table 5.2-2 shows the new bare direct cost (BDC), total capital cost (TCC), annual costs and the cost of electricity produced (COE).

5.2.1 Comparison of "Greenfield DEMO" with "SIRIUS-M Upgrade DEMO"

5.2.1.1 The Advantage of Electric Power Conversion for the SIRIUS-M ETR

It may be economically viable to produce part (or all in the 100 MJ case) of the laser input power requirements by adding electric conversion equipment. The cost impact of this option on the affected facility items is shown in Table 5.2.1-1 for the 13.4 MJ, 2 m, 10 Hz design. The added cost is relatively modest, $31 M, in order to supply about 60% of laser input requirements (for a 10% efficient, 1 MJ laser). This will result in the decrease in the cost of electricity charged to the facility and a slight increase in the O&M cost. The plan should go ahead if the difference in the FOM is below zero,

Table 5.2-1. Cost Difference, ΔC in $M for Affected Items for the DEMO

Item	4 m, 100 MJ, 10 Hz ETR	Demo	ΔC	
Electrical plant	62.9	80.6	17.7	
Turbine plant	0	96.6	96.6	
Heat rejection	28.2	21.4	- 6.8	
Cooling structures	8.2	7.4	- 0.8	
TOTAL			+106.7	(+15.7%)

Table 5.2-2. Various Costs for the DEMO Plant

Item	Value
BDC ($M)	787
TCC ($B)	1.93
Annual Costs in $M	
(Investment return	138.)
O&M	44.7
Fuel	0
COE, with investment return, ¢/kWh	7.6
COE, w/o investment return, ¢/kWh	1.9

Table 5.2.1-1. Cost Difference, ΔC for Affected Items in the 13.4 MJ, 2 m, 10 Hz Facility

Item	ΔC, $M
Electric plant	+13.8
Turbine plant	+19.3
Heat rejection	- 1.5
Cooling structures	- 0.4
	+31.2

Table 5.2.1-2. ΔFOM Table

The figures represent the reduction (if negative) or increase (if positive) in yearly cost of owning and operating the facility (in $M) depending on which figure of merit (FOM) is used.

Cost of Electricity ¢/kWh	FOM_0 Logic	FOM_1 Logic
3	-0.58	2.16
6	-8.8	-6.1

because then the savings in the electricity cost outweigh the additional O&M cost and the additional prorated capital cost (which is defined differently for the alternative FOM discussed above). The results are presented in Table 5.2.1-2 (negative figures represent annual savings in $M in operating and ownership costs) for the two cases of the cost of electricity (3¢/kWh and 6¢/kWh) and the two figures of merit used (the alternative FOM is FOM_1). The FOM's are defined in 2.2 and 4.2. We see that for 6¢/kWh, the electric conversion equipment should be included (for a yearly savings of ~ $6 M in case of of FOM_1, ~ $9 M in case of FOM_0). In case of 3 ¢/kWh electricity, the FOM_0 decision gives very small advantage to electric conversion, whereas FOM does not; this may change (in favor of electric conversion) if laser waste heat is used for feedwater heating, thus increasing the amount of electric power available.

Similarly, the corresponding information for a 100 MJ, 4 m, 10 Hz ETR is shown in Tables 5.2.1-3 and 5.2.1-4. In this case, all of the laser input power is supplied by the electric conversion equipment and a substantial amount of electric power is sold outside the facility. It can be seen that in this case, too, it is economically advantageous to convert to electric power on site, because of the high electricity demand of the laser input power equipment.

5.2.1.2 The Advantages of a 4 m ETR and Upgrade DEMO vs. a 2 m ETR and a Greenfield DEMO

It has been decided that a 2 m, 13.4 MJ, 10 Hz ETR with breeding will be the base case for the SIRIUS-M facility. Similarly we have looked at the cost estimate of a 366 MWe DEMO plant, assuming a similar configuration (except for larger cavity), T_2 self-sufficiency and also comparing the direct cost to that

Table 5.2.1-3. Cost Difference, ΔC for Affected Items in the 100 MJ, 4 m, 10 Hz Facility

Item	ΔC, \$M
Electric plant	+ 14.6
Turbine plant	+ 113
Heat rejection	- 10.4
Cooling structures	- 1.3
	+ 115.9

Table 5.2.1-4. ΔFOM Table for the 100 MJ, 4 m, 10 Hz Facility

The figures represent the reduction (if negative) or increase (if positive) in yearly cost of owning and operating the facility (in \$M) depending on which figure of merit (FOM) is used.

Cost of Electricity ¢/kWh	FOM_0 Logic	FOM_1 Logic
3	-33.1	-22.9
6	-94.6	-84.4

of a 4 m, 100 MJ ETR. It can be seen in Tables 4.2-3 and 4.2-4 that, if uncertainties in cost estimates are neglected, some 4 m design options can compete with a 2 m ETR based on our figures of merit. It will be shown here, that if the total cost of an ETR and a subsequent DEMO are considered, it may be advantageous to start with a 4 m, 100 MJ ETR and upgrade it to a DEMO, rather than to have a 2 m, 13.4 MJ ETR and subsequently build a separate DEMO.

In Section 2.2 and Fig. 2.2-1, it was shown that a 4 m, 100 MJ ETR with a rep rate of ~ 10 Hz was possible, and it can be seen that it is economically advantageous to go to higher rep rates because the FOM decreases (the lower the FOM the better). This will also have an impact on the total life of the ETR facility, because the required cumulative damage will be achieved in a much shorter time (about 5 years instead of 10 years), so the schedule for a DEMO can be advanced.

In Subsection 5.2.1.1 we have shown that it is economically advantageous to add electric power conversion equipment to a 100 MJ, 10 Hz ETR. In addition, it can be said that the electric power conversion equipment won't add to engineering uncertainty of the facility, and won't significantly add to its unavailability (availability of this equipment is on the order of 90% from conventional plant experience, and assumed availability of SIRIUS-M ETR is ~ 50%).

Therefore, we can look at a 100 MJ, 4 m, 10 Hz ETR that, after retirement and after certain equipment is replaced becomes a DEMO. This combination will cost less than building a 2 m ETR and a DEMO separately.

The equipment to be replaced at the end of life will be the following:

- The reactor cavity, due to damage, new knowledge gained from operating the ETR and a possibly different cooling/breeding medium.

- Breeding equipment due to different breeding medium and extraction method of T_2. In this case, just the equipment responsible for extraction of T_2 is replaced.
- Laser power supply due to wear and tear of the high voltage, high total pulse number equipment.
- Laser optics, due to radiation damage.
- Possibly heat transfer equipment if the ETR is using H_2O cooling and the DEMO is using liquid metal cooling (we are looking at the worst case here). H_2O cooled DEMO is the base case.

Excluded is the normal replacement of equipment that is included in the ETR's and DEMO's annual O&M costs.

The direct cost of these items is shown in Table 5.2.1-5. The items that will not need replacement are the buildings, the heat rejection plant, the electrical plant exclusive of the laser power supply, the turbine plant, miscellaneous plant, part of the laser excluding the optics, the target factory, the pellet injector (a minor item), the vacuum system, isotope separation and storage, Xe recycle equipment, fuel storage, any water cooling outside the first wall and the reflector, instrumentation and control and maintenance equipment.(1)

Table 5.2.1-6 shows the comparison of a 4 m, 100 MJ 10 Hz ETR and a 2 m, 13.4 MJ, 10 Hz ETR. Note that credit is given for excess electricity produced in the former. Also, there are two lifetime costs for the 100 MJ, 4 m ETR: one corresponding to the original 10 year lifetime and the other corresponding to the 6 year lifetime whereby credit is taken for the higher damage rates of the enhanced target facility and the slightly lower availability due to the electric power conversion equipment. Also given are the total lifetime costs

Table 5.2.1-5. Items to be Replaced at End of 100 MJ, 4 m, 10 Hz ETR Life

Item	Direct Cost ($M)
Reactor Cavity	~ 140
Breeding Equipment (extraction of T_2)	5
Laser Power Supply	31.7
Laser Optics	33
Heat Transfer Equipment	102.8
Total	313
ΔTOC	592

Table 5.2.1-6. Comparison of Enhanced Target (4 m) ETR Plus Upgrade Demo and a Baseline (2 m) ETR Plus Greenfield Demo Combinations

Type Cost	Value for 4 m ETR ($M)	Value for 2 m ETR ($M)
BDC	787	450
TOC	1488	850
O&M	45	25
Fuel	0	36[c] 0
Electricity[a]	-48 (-96)[a]	13
Total Annual Cost	~ 0 (-50)[a]	75[c] 38
Total Lifetime Cost		
N = 10 y	1488(1000)[a]	1605[c] ~ 1200
N = 6 y[b]	1488(1188)[a]	
Total Lifetime Cost		
ETR + Demo	2080(1780)[a]	3100[c] 2700 (3000)[c,d] (2600)[d]

(a) Electricity sold at 3¢/kWh (6¢/kWh); bought at 3¢/kWh for the 2 m ETR.

(b) Includes reduction in availability due to electric conversion equipment and an increase in the damage rate due to enhanced target and 10 Hz rep rate.

(c) This case assumes no breeding of T_2 for the 2 m ETR. The next column includes breeding.

(d) Numbers in parentheses assume electricity production to meet part of the laser demand in the 2 m ETR case.

of the ETR + DEMO combinations; separate ETR and DEMO in case of the 2 m, 13.4 ETR and a DEMO built on an earlier ETR in case of the 4 m, 100 MJ ETR. It can be seen that this latter case has a much lower lifetime cost and therefore should be seriously considered. Even if we compare just the two ETR's, we can see that if the cost of electricity is 6¢/kWh or higher, the enhanced target ETR is less expensive over the lifetime than our baseline ETR. This is due to the substantial credit from electricity sold outside the facility.

Reference for Chapter 5

1. Zoran Musicki, "The Economic Analysis of SIRIUS-M, A Symmetrically Illuminated Inertial Confinement Fusion Engineering Test Reactor," UWFDM-708, September 1986.

6. DESCRIPTION OF A 92 BEAM ILLUMINATION SYSTEM

Up until FY'87 we had been using 32 beams for the reference case. The group at LLE which has been studying target performance as a function of uniformity of illumination for many years has concluded that 32 beams may not be adequate and have suggested that we use 96 beams.

Having obtained the coordinates for a 96 beam distribution and investigated the layout in spherical geometry, we were unable to arrive at a configuration which allowed a reasonable blanket design adapted to it. We then began to investigate other options and found a 92 beam configuration that appears to be more suitable. Using the 92 beam system, the spherical cavity is divided into 80 hexagonal and 12 pentagonal modules with a beam in the center of each one. The configuration is based on the icosahedron platonic solid which is composed of 20 equilateral triangles with 12 points where the triangles' vertices meet. Each of the pentagonal modules is located at a vertex confluence point (12 of them) and is surrounded by five hexagonal modules making a cluster of six modules. Further, there are another 20 hexagonal modules located between these clusters. The length of each hexagonal module side is identical to a pentagonal module side.

Figure 6-1 shows a cluster of one pentagonal module and five hexagonal modules as viewed from inside and outside the cavity. From inside the cavity one sees a closed configuration where the modules meet. Here the protective tiles will present a closed front to the ions and target debris. From the back of the cavity one observes large gaps between the modules. These gaps will contain the structure of the frame which will hold the modules together.

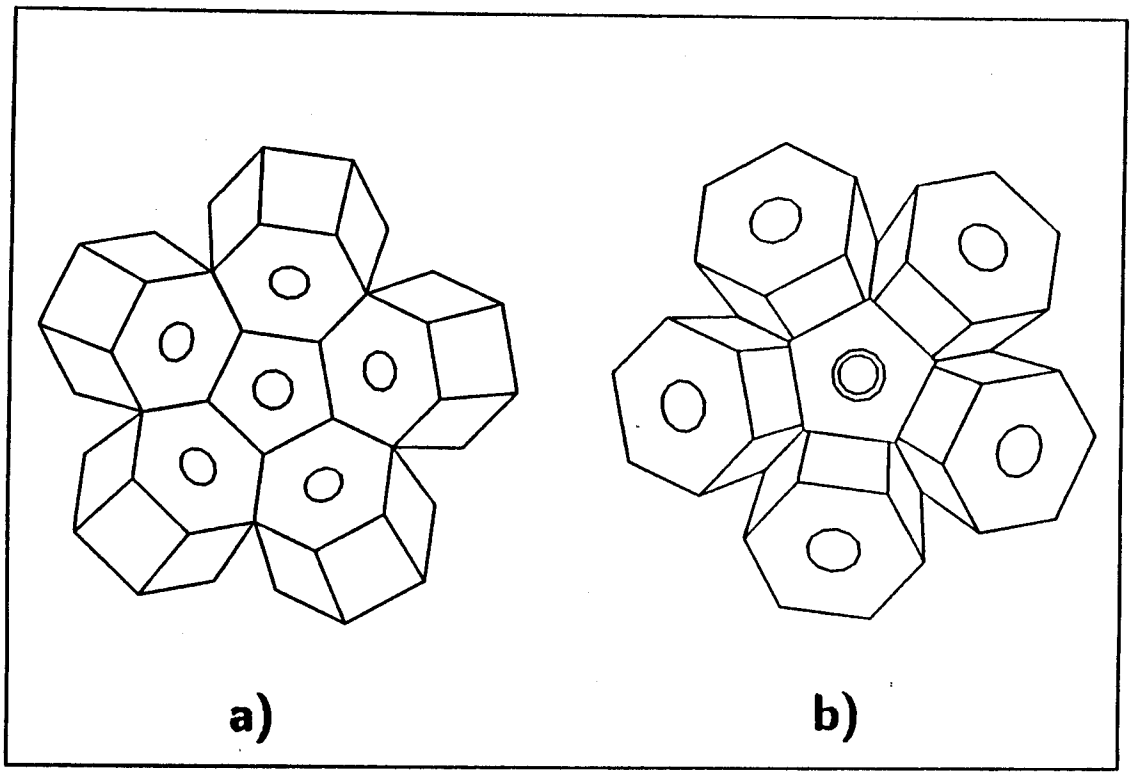

Fig. 6-1. A cluster of one pentagonal and five hexagonal modules oriented to conform to a spherical geometry: a) view from inside the sphere and b) view from outside the sphere.

The modules will be tapered from the back to the front for easy insertion and removal from the structural frame. Each module will have a graphite protective tile supported on a collar which fits into the beam port. Coolant connections are made in the back of the module. Thus, each module is completely self-contained and independent of its neighboring modules. Maintaining these modules should be straightforward.

Figure 6-2 is a cross section of the reactor containment building showing the cavity in the center. Although there are 92 uniformly distributed beams, only 12 show up in this cross section. With the exception of the larger number of beams, the rest of the design is the same as earlier.

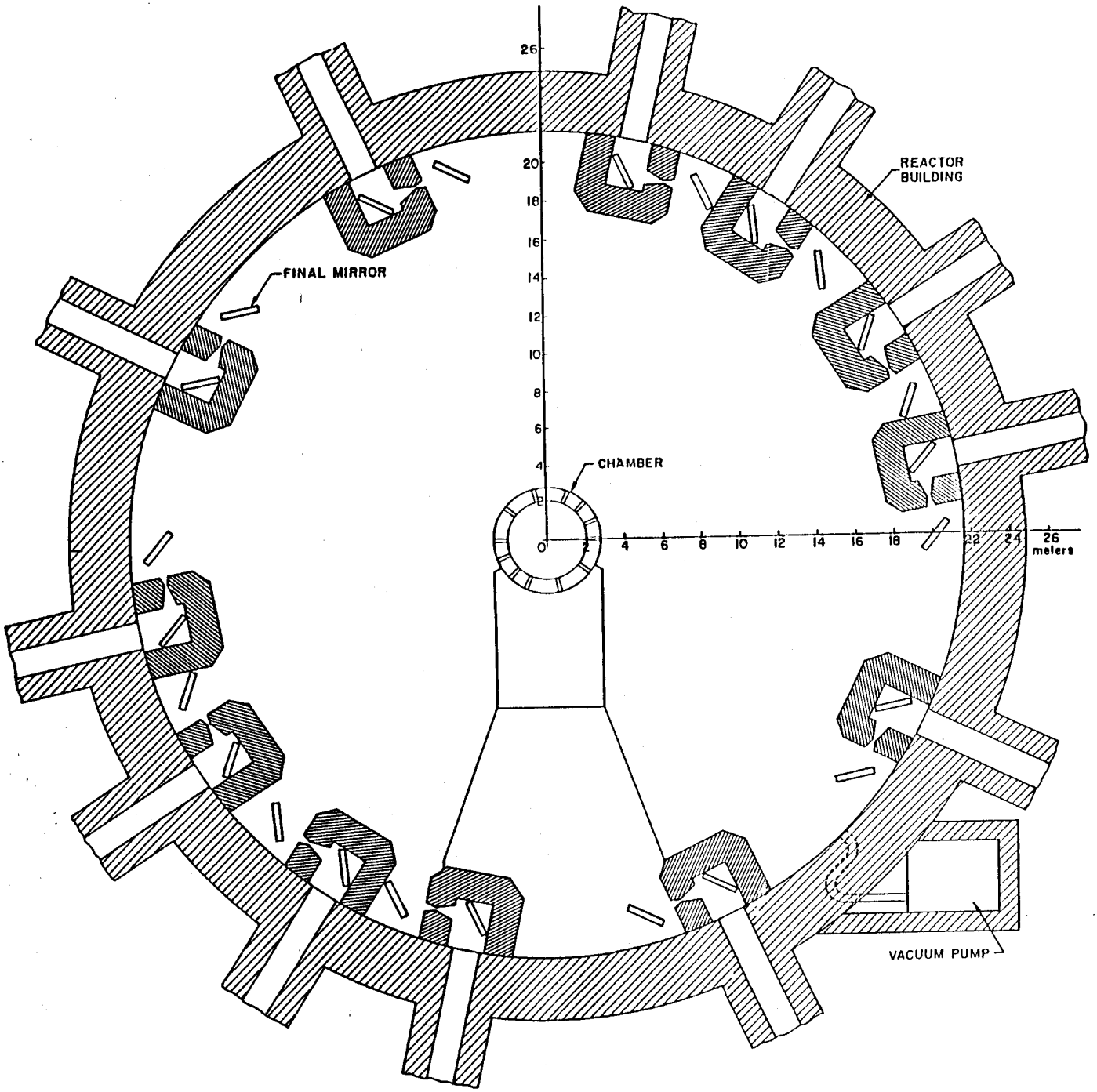

Fig. 6-2. Cross section of SIRIUS-M reactor building with 92 symmetrically distributed beams.

7. SUMMARY AND CONCLUSIONS

Based on the tasks performed on SIRIUS-M during FY 87 we can make the following conclusions:

1. Having performed a study of nine options using variation in materials, material compositions, dimensions and design we conclude that T_2 breeding is possible in SIRIUS-M with very little degradation in damage in the material test modules. T_2 self-sufficiency can be achieved by the simple addition of $LiNO_3$ to the cooling water and utilizing a front multiplier zone of either Pb or Be. A substantial saving of 433 M$ is realized over the lifetime of the reactor resulting in a reduction of 8% in the radiation damage figure of merit given in M$/dpa.
2. A crossover in the laser beams at the containment building boundary is needed to reduce neutron streaming. We find that with a 1 MJ Kr laser split into 92 beams, each focused at the crossover to 1.0 cm diameter, the energy density is 10^{13} W/cm^2. The threshold for breakdown due to multi-photon absorption is 2 x 10^{13} W/cm^2 and due to cascade breakdown 2.5 x 10^{15} W/cm^2. Based on this, we do not expect breakdown to occur. Further, increasing the number of beams to 92 and reducing the focal aperture from 10 cm to 2 cm, reduces the dose to the windows by a factor of 25, with an end of life dose of only 0.01 Mrad.
3. We have investigated the possibility of using an enhanced performance 100 MJ target instead of the original 13.4 MJ for SIRIUS-M. We find that the target chamber must increase to 4 m radius, the direct costs increase by 21%, the lifetime costs by 2.5%, and the radiation damage figure of merit goes from 12 to 13 M$/dpa. There appears to be no incentive to go to a 100 MJ target for SIRIUS-M.

4. In scaling SIRIUS-M to a DEMO, we have used two methods. The so-called "Greenfield DEMO" which means a facility started from ground zero, was compared to an upgrade of SIRIUS-M, where the cavity was replaced and necessary auxiliary equipment added to make it qualify as a DEMO. We have found that almost a B$ can be saved by upgrading a SIRIUS-M facility to a DEMO, over a "Greenfield DEMO."
5. A 92 beam illumination system was developed in response to assertion that 32 beams provided marginal uniformity. This system is very compatible with incorporation of a breeding blanket into the cavity and allows a straightforward maintenance scheme. It is based on the distribution in an icosahedron platonic solid consisting of 20 equilateral triangles whose vertices converge at 12 points. The blanket consists of 80 hexagonally shaped and 12 pentagonally shaped modules, each with a beam port in its center. The modules are supported within a structural frame and are entirely self-sufficient and independent of each other. All the other aspects of the design are the same as in the 32 beam case.